Nanolime, nanosilica or ammonium phosphate? Laboratory and field study on consolidation of a byzantine marble sarcophagus

(Article begins on next page)

22 November 2024

NANOLIME, NANOSILICA OR AMMONIUM PHOSPHATE? LABORATORY AND FIELD STUDY ON CONSOLIDATION OF A BYZANTINE MARBLE SARCOPHAGUS

Enrico Sassoni[1,*], Greta Ugolotti[2], Michele Pagani[2]

[1] Department of Civil, Chemical, Environmental and Materials Engineering, University of Bologna, Via Terracini 28, 40131, Bologna, Italy

[2] Department of Cultural Heritage, University of Bologna, Via degli Ariani 1, Ravenna, Italy

* Corresponding author: enrico.sassoni2@unibo.it

ABSTRACT

The present paper aims at comparing commercial nanolime and nanosilica dispersions with an aqueous solution of diammonium hydrogen phosphate (DAP) for consolidation of marble. The consolidants were first tested in the laboratory on artificially and naturally weathered marble specimens. The DAP-treatment applied by poulticing outperformed nanolime and nanosilica in terms of consolidating effectiveness, while showing good compatibility with the substrate. After preliminary testing of all the three consolidants on small areas of a byzantine marble sarcophagus, the DAP-treatment applied by poulticing was finally selected for application onto the whole sarcophagus. Field results confirmed the promising performance of the DAP-treatment.

KEYWORDS

Nanotechnology; Nanoparticles; Consolidant; Calcium hydroxide; Colloidal silica; Hydroxyapatite; Calcium phosphate; Marble; Field-testing; Non-destructive tests

HIGHLIGHTS

➢ Nanolime, nanosilica and ammonium phosphate were compared as marble consolidants
➢ In the laboratory, they were tested on artificially and naturally weathered samples
➢ In the laboratory, ammonium phosphate was more effective than the nanoconsolidants
➢ The three consolidants were then tested on a byzantine marble sarcophagus
➢ Field results confirmed the high potential of the ammonium phosphate treatment

1. INTRODUCTION

Nanoconsolidants, such as nanolimes and nanosilica, have received a lot of attention in recent years, because they exhibit several advantages compared to traditional consolidants.

Nanolimes are colloidal dispersions of Ca(OH)$_2$ nanoparticles in alcohol (typically ethanol or isopropanol). After being introduced into the substrate to be consolidated, Ca(OH)$_2$ nanoparticles undergo carbonation by atmospheric CO$_2$, thus forming CaCO$_3$ with binding capacity. In the first pioneer study by Baglioni and co-workers [1], dispersion of Ca(OH)$_2$ particles in short-chain aliphatic alcohols was proposed to overcome the limitations of traditional aqueous solutions ("limewater") and aqueous suspensions ("milk of lime" or "limewash") of Ca(OH)$_2$ particles, which typically exhibit low penetration depth, low effectiveness and tendency to form white hazes on the treated surface. By using alcohol instead of water as dispersion medium, high colloidal stability could be achieved, thanks to electrostatic and hydrophobic interactions that prevent particle aggregation and sedimentation [1]. This allowed to increase the concentration of Ca(OH)$_2$ particles compared to limewater and limewash, with a consequent increase in the consolidating effectiveness [1,2]. While in the cited pioneer study Ca(OH)$_2$ particles exhibited both nano- and micro-size, so they could not be strictly considered as "nanolimes", the same research group later developed and patented methods to synthetize proper Ca(OH)$_2$ nanoparticles (with size below 500 nm), as described in more detail in the review paper [2]. In the following years, several studies have investigated the effects of various parameters on the treatment performance. In particular, the solvent used as dispersion medium was proven to significantly influence the penetration depth [3-6], the carbonation process [7] and the mineralogical composition of CaCO$_3$ resulting from nanolime carbonation [8]. In fact, Ca(OH)$_2$ nanoparticles dispersed in alcohols are not inert, as initially believed, but partially transform into calcium alkoxides (calcium ethoxide or isopropoxide in the case of dispersion in ethanol or isopropanol, respectively) [8]. This leads to undesired effects, namely a reduction in the rate of transformation into calcium carbonate and formation of metastable calcium carbonate phases (vaterite and aragonite) [2,8]. The consolidating effectiveness and the compatibility of commercial and laboratory-developed nanolimes have been investigated on a variety of substrates, including limestone [4,7,9-13], marble [13,14], dolostone [3,13], sandstone [2,7], granites [12], lime-based mortars [6,10,15,16] and wall paintings [3,17], as well as paper [2], canvas [2], wood [2] and archaeological bones [18]. Depending on the porosity of the substrate, the particle size distribution and the dispersion medium, nanolimes can reach a high penetration depth (up to 40 mm in the case of highly porous limestone [4]), but they may be transported back to the surface during drying, with the risk of particle accumulation near the surface [4]. As a consequence, a fair consolidating effectiveness has been reported in several studies (in terms of material loss after peeling test [6,7,13,14], microdrilling resistance [6,10], ultrasonic pulse velocity [14,15], compressive strength [16] and resistance to salt weathering [9,11,19]), but cases of over-strengthening of the surface [10] and lack of consolidation of the substrate [2] have been reported as well. In general, nanolimes have been found to cause modest pore occlusion [6,10,12] and limited alterations in water transport properties [6,9,10,12]. In terms of aesthetic compatibility, even though satisfactory results have been generally found [3,9,12,14], cases of visible whitening have been also reported [2,6,10,13].

Consolidants based on nanosilica are colloidal dispersions of SiO$_2$ nanoparticles in water. After being introduced into the substrate, during drying hydroxyl groups present on the nanoparticle surface condense, with release of water molecules and formation of Si-O-Si bonds that allow for bonding of the consolidant to the substrate [20], if the substrate has OH$^-$ surface groups. Compared to traditional consolidants based on ethyl silicate,

nanosilica dispersions have the advantage of requiring curing for a much shorter time: only a few days are needed for gelation of silica nanoparticles, while several months are needed for hydrolysis of ethyl silicate and subsequent condensation [21]. Differently from ethyl silicate, nanosilica dispersions do not cause hydrophobization of the treated substrate (because no hydrophobic ethoxy groups are present) and can be applied also on moist substrates and in very humid environment, even though the consolidating effectiveness has been proven to be higher in dry environment [22]. However, unlike ethyl silicate, nanosilica generally exhibits limited ability to penetrate deeply into the substrate: accumulation near the treated surface [23,24] and formation of a thick surface crust [9,12] have been frequently reported, even though a penetration depth as high as 30 mm has been found in the case of highly porous stone [22]. The effectiveness and the compatibility of nanosilica dispersions have been evaluated on several types of substrate, including limestone [9,11,20,23,24], calcarenite [22], tuff [25] and granite [12]. As a consequence of the limited penetration depth, the consolidating effectiveness of nanosilica dispersions has been found to be generally modest [9,11,12,23], although some improvement in mechanical properties has also been reported [22,25,24]. After treatment, porosity reductions by 10%-30% [12,24] have been found, with consequent decreases in water capillary absorption by 10-70% [20-24] and water vapor permeability by 25-75% [20,24]. As for aesthetical compatibility, a low color change has been reported in some cases [22-24] but several studies pointed out an unacceptable color change after treatment [12,20].

In spite of the abundant literature on the performance of nanolimes and nanosilica on porous carbonate substrates, such as limestones [4,7,9-12,20,22-24] and lime-based mortars [6,10,15,16], only very few studies have investigated the performance of these nanoconsolidants on marble [13,14]. Marble is often in need of consolidation because it is highly sensitive to thermal weathering induced by temperature excursions [26]. In fact, calcite grains constituting marble (as well limestones and lime-based mortars) undergo anisotropic deformation upon temperature variations, expanding parallel and contracting perpendicular to the crystallographic c axis [26]. Whereas in porous limestones and mortars thermal deformation of calcite crystals can be accommodated by voids among the grains [27], this is not the case in fresh marble, where grains are very tightly packed and virtually no voids exist with among them [26]. As a consequence, thermal deformation of calcite grains leads to stress at the grain boundaries, which results in grain separation and microcrack formation [26]. This process is responsible for the macroscopic "sugaring" (i.e. grain detachment and loss) and bowing (i.e. warping of thin slabs) often affecting marble [28]. To arrest grain loss and bowing, consolidation of marble elements is hence often necessary [29,30].

For consolidation of weathered marble, many products have been tested through the years, but all traditional consolidants have shown limitations, including organics (lacking compatibility with the substrate and stability over time [31]), limewater (having low effectiveness [31,32]) and silicate consolidants (lacking chemical bonding to the substrate [33] and hence significant effectiveness [34]). A novel type of consolidant for marble and carbonate substrates in general was proposed in 2011, namely diammonium hydrogen phosphate (DAP) [35,36]. DAP is dissolved in water to obtain aqueous solutions that are applied onto the carbonate substrate, so that PO_4^{3-} ions from the solution and Ca^{2+} ions from the substrate (and/or externally added to the phosphate solution [37]) react to form new calcium phosphates, according to the following reaction [38]:

$$10CaCO_3 + 5(NH_4)_2HPO_4 \rightarrow Ca_{10}(PO_4,CO_3)_6(OH,CO_3)_2 + 5(NH_4)_2CO_3 + 3CO_2 + 2H_2O \quad (1)$$
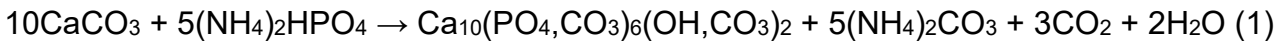
Calcium phosphates formed by reaction (1) crystallize at the boundaries among calcite grains, thus bridging them, increasing cohesion and improving mechanical properties [35]. Ideally, the product of reaction (1) is hydroxyapatite (HAP, $Ca_{10}(PO_4)_6(OH)_2$), which is the most stable calcium phosphate mineral at pH>4 [39]. However, as reported in reaction (1), HAP formed in the presence of abundant CO_3^{2-} ions (coming from the carbonate substrate and/or from atmospheric CO_2) is typically not stoichiometric, with CO_3^{2-} ions entering the crystal structure and replacing OH^- ions (A-type substitution) and/or PO_4^{3-} ions (B-type substitution) [40]. Moreover, alongside HAP also other calcium phosphate minerals may form, such as octacalcium phosphate (OCP, $Ca_8(HPO_4)_2(PO_4)_4·5H_2O$) and brushite ($CaHPO_4·2H_2O$), depending on the reaction conditions (pH, degree of supersaturation, etc.) [35,40-42]. While formation of OCP, which is less soluble than calcite, is not expected to negatively affect the treatment success [37], formation of minerals that are more soluble than calcite (such as brushite) should be prevented. Since the DAP treatment was proposed, several studies have investigated the influence of various reaction parameters, such as the concentration of the DAP solution [35,37,42-44], its pH [36,44,45], the treatment duration [35,37,41], the addition of external ions (Ca^{2+} [37,46], Sr^{2+} [37,44], Mg^{2+} [37,44], Al^{3+} [44], CO_3^{2-} [37]) and the addition of organic solvents to the DAP solution [44,45]. The consolidating ability of DAP has been assessed on a multiplicity of substrates, including marble [29,45], limestone [35,36,47-51], sandstone [52,53], calcarenite [53], lime-based mortars [54,55], cement-based mortars [55], gypsum stuccoes [56], concrete bricks [57] and archaeological bones [18,58,59]. Thanks to the low viscosity of the DAP solution, a good ability to penetrate deeply into the substrate has been generally reported, the penetration depth of the solution reaching 40 mm in mortars [55] and 50 mm in highly porous limestone [43]. The consolidating capacity has been demonstrated in several studies, in terms of ultrasonic pulse velocity [29,35,37,45,49,53,60], tensile strength [35,49,52], compressive strength [55,61], resistance to abrasion [29,49], resistance to material loss by peeling [29,62,63], microdrilling resistance [36,51], resistance to freeze-thaw cycles [50,60] and salt crystallization cycles [50,60,62]. DAP solutions have been found to have similar and often superior consolidating capacity compared to alternative consolidants, such as nanolimes [60,63] and ethyl silicate [49,50,53]. Compared to these alternatives, DAP solutions have the advantage of being effective after just 24-48 hours [64], instead of several weeks like nanolimes [2] or several months like ethyl silicate [21]. Newly formed calcium phosphates generally cause limited alterations in porosity and leave the treated substrate hydrophilic, with consequent slight alterations in water and water vapor transport properties [64]. The lack of any hydrophobization of the treated substrate (unlike the case of ethyl silicate [21]) and the absence of any toxic compound [49] are further elements that strengthen the potential of the DAP treatment. Furthermore, in the case of marble, alongside the consolidating action [29,45,65], a significant protective ability has also been assessed [44,45,66,67]. Indeed, HAP is significantly less soluble than calcite, hence the formation of a continuous, crack-free and pore-free coating of HAP over the marble surface can protect it from dissolution in rain [46]. Finally, a further important aspect is that the DAP-treatment, although not reversible, fulfils the requirement of retreatability. In fact, as is the case for all inorganic consolidants, the new mineral formed after consolidation cannot be dissolved and removed (the low solubility and high stability of HAP actually ensure the treatment durability); however, because the newly formed HAP

leaves the stone hydrophilic and does not occlude pores, the possibility to retreat the stone in the future by either the same or a different consolidant is guaranteed [49].

Even if the potential of the DAP treatment has been extensively demonstrated in laboratory studies, the adoption of this treatment for consolidation of real artworks in the field is currently still limited, for two main reasons:

1) Several studies have compared the performance of the DAP treatment with ethyl silicate [30,49,50,52,53,68], but only in a few cases the DAP treatment has been compared to nanoconsolidants [60,63], which are nowadays attracting a lot of attention. A direct comparison among these treatments, with the possibility to highlight pros and cons of each alternative, would actually be very useful for practitioners who need to select the most appropriate product for application onto real artifacts;

2) Several cases of application of the DAP treatment onto real buildings and monuments have been reported in the literature [69-72], but only in a limited number of cases systematic data on the treatment performance are available [71,72]. Scientific studies on the application and the assessment of innovative treatments on real buildings are actually very important to guide the selection and the application of these treatments in other cases. Notwithstanding valuable attempts to replicate in laboratory studies the substrate conditions (e.g., presence of soluble salts, bioorganisms, previous conservation treatments) and the environmental conditions (e.g., variations in relative humidity, temperature, solar radiation) that may be present in the field [11,19,68,73,74], still only field studies can account for the complexity of real situations, where all the above mentioned factors act simultaneously [75-78].

Therefore, the aim of the present study is to contribute to overcome the two limiting factors described above, by comparing the effectiveness and the compatibility of nanolimes, nanosilica and DAP for consolidation of weathered marble, both in laboratory and in a real case study. The three consolidants were regarded as reasonable candidates for application onto marble, considering that: (i) nanolime and DAP were actually developed for consolidation of carbonate substrates; (ii) nanosilica has been reported to be fairly effective on carbonate substrates [22,24], although its performance is expected to be lower than in the case of silicate stones, just like ethyl silicate [21]. The present study was in particular articulated as follows:

1) A comparison was carried out in the laboratory, to evaluate the effectiveness and the compatibility of commercial dispersions of nanolime and nanosilica and a laboratory-prepared DAP solution for consolidation of weathered marble specimens. For laboratory testing, two groups of specimens were used, one group being artificially weathered and one being naturally weathered, with the aim of obtaining laboratory results as representative as possible of real conditions in the field;

2) The three consolidants were then applied on small areas of a real marble artwork and the effectiveness and aesthetic compatibility of the treatments were evaluated. Based on the results of the comparative tests performed both in the laboratory and in the field, the DAP treatment was finally selected for application onto the whole marble artwork and the resulting performance was evaluated. The artwork selected for field-testing was a byzantine marble sarcophagus in the garden of the Church of St. Vitale in Ravenna (Italy, VI century), which belongs to the UNESCO World Heritage List.

2. MATERIALS AND METHODS

2.1. Marble substrates

The specimens for laboratory testing were selected with the aim of resembling as closely as possible the conditions of the byzantine marble sarcophagus that was the object of field-testing. To this aim, the marble sarcophagus was first analyzed and the laboratory specimens were later prepared based on the obtained results, as described in the following.

2.1.1 Byzantine marble sarcophagus

The marble sarcophagus that was the object of field-testing is situated in the garden of the Church of St. Vitale in Ravenna (Italy), as illustrated in Figure 1. The Church of St. Vitale dates back to the VI century and is a masterpiece of early Christian byzantine architecture, enlisted in the UNESCO World Heritage List since 1996. The sarcophagus most probably dates back to the beginning of the VI century [79]. Today, it is known as the "Sarcophagus of the Spreti Family", as it was used to bury the members of the noble Spreti family from the XVI to the XX century. It was moved to the current location in 1923.
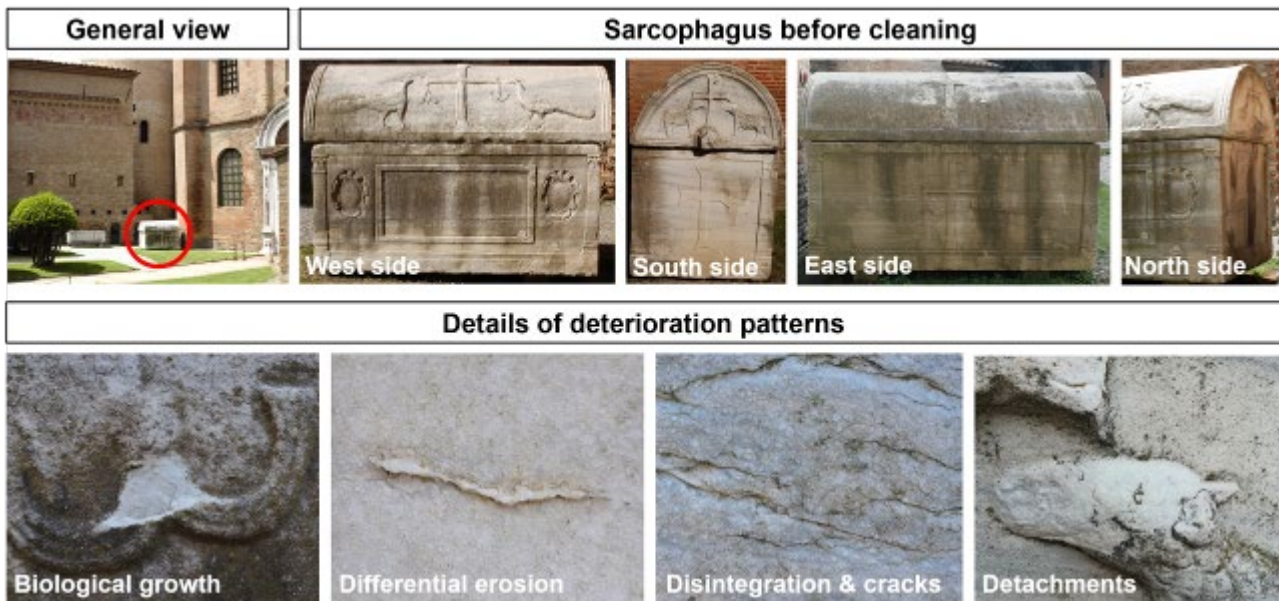
Figure 1. General view of the sarcophagus and details of the deterioration patterns.

Previous studies [79] and direct petrographic analyses (not reported here) indicate that the sarcophagus is made of Proconnesian marble, quarried in the Marmara Island (Turkey), known in ancient times as Proconnessos. The fact that the sarcophagus is made of marble quarried thousands of kilometers away is not surprising, as in ancient times rough artifacts were commonly shipped overseas and, in particular, sarcophagi made of Proconnesian marble were diffused in all the territories of the Roman Empire [79,80]. The use of

Proconnesian marble became so common that, even in Rome, it progressively replaced Carrara marble (quarried much closer) and almost reached 100% of the marbles used in the Antonine and Severian periods [80].

In general, Proconnesian marble is a calcitic marble with minor presence of dolomite, micas, apatite and pyrite, as well as organic impurities [80,81]. It has medium to large grain size, with maximum grain size ~2 mm [80,81]. Visually, it is white with regular greyish bands composed of fine-grained calcite [81], characteristic of Proconnesian marble.

At the beginning of 2019, the sarcophagus exhibited severe weathering, as illustrated in Figure 1. First, marble was largely affected by biological growth, covering almost the whole surface. Small lichens, green to orange in color, were present over a homogenous dark patina. The cover of the sarcophagus was apparently less affected by biological growth but in turn, being directly exposed to rain washout, was severely affected by dissolution of calcite grains. Calcite dissolution led to differential erosion of the marble surface, clearly visible where less soluble veins were present. Both the cover and the lower part of the sarcophagus were also affected by diffused disintegration, triggered by thermal weathering and growth of microorganisms, which resulted in formation of intergranular fissures and grain loss. In some cases, disintegration and cracking led to the detachment of centimetric marble fragments.

A small fragment, which had detached from the sarcophagus and would have been impossible to re-attach, was analyzed by scanning electron microscopy (SEM, Philips XL30). The surface morphology and the grain size of the Proconnesian marble constituting the sarcophagus are illustrated in Figure 2.
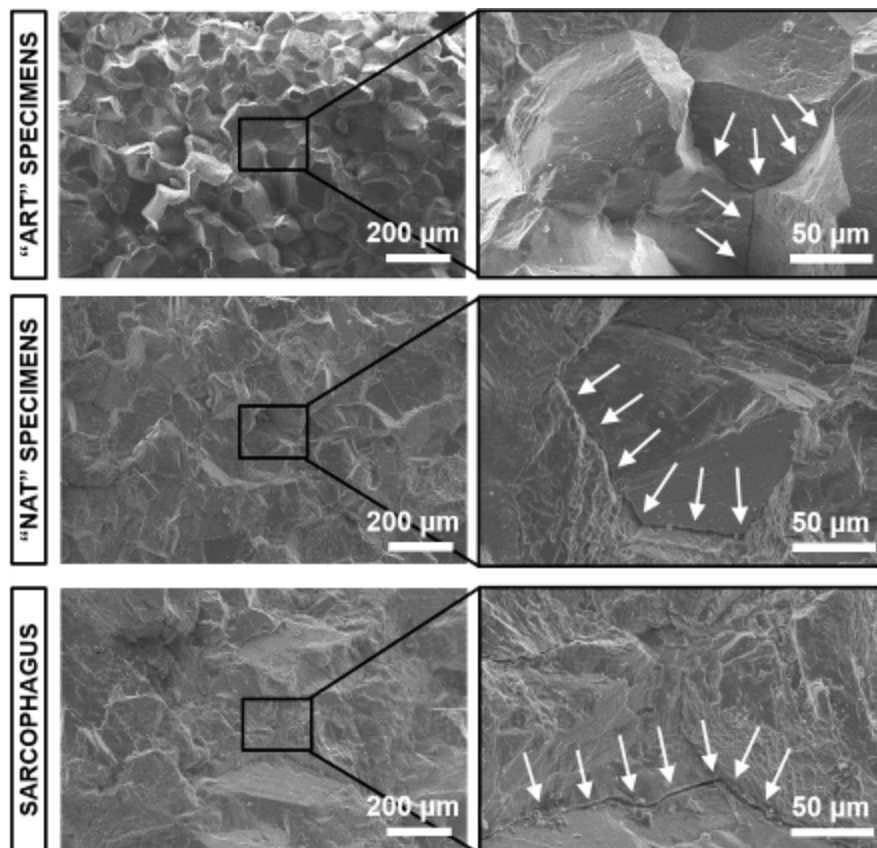
Figure 2. SEM images of artificially ("ART") and naturally ("NAT") weathered marble specimens, in comparison with the Proconnesian marble constituting the sarcophagus (arrows indicate cracks).

2.1.2   Laboratory specimens

For laboratory testing, two groups of specimens were considered (10 specimens for each group), as described in the following.

With the aim of testing the consolidants on marble specimens that exhibited intergranular decohesion (like the sarcophagus, Figure 2) but were free from contaminants that may alter the expected chemical reactions (e.g., soluble salts, microorganisms, residues of previous interventions), artificially weathered specimens (labelled as "ART") were used. First, small slabs ($5 \times 5 \times 2$ cm^3) were sawn from a single slab of fresh Carrara marble (supplied by Imbellone Michelangelo s.a.s., Italy). Then, the "ART" specimens were obtained by heating the small slabs in an oven at 400 °C for 1 h, according to a previously developed method [35]. In this way, the anisotropic deformation of calcite crystals upon heating was exploited to induce microcrack formation and grain disaggregation, by accelerating the process that occurs in the field after prolonged exposure to temperature excursions [28].

With the aim of resembling the condition of the sarcophagus, exhibiting both grain decohesion and biological growth, naturally weathered specimens (labelled as "NAT") were also used. A slab of naturally aged calcitic marble, severely affected by biological growth (Figure 3), was first cleaned by different methods (the same methods later used on the sarcophagus, cf. § 2.3.1) and then sawn into 10 specimens ($10 \times 4 \times 2$ cm^3). Because the various parts of the slab initially exhibited differential biological deterioration and were cleaned by different methods, the 10 "NAT" specimens had slightly different initial properties (in terms of color, porosity, possible residues of microorganisms and/or cleaning products, etc.) when the consolidants were applied.

Compared to the Proconnesian marble constituting the sarcophagus, the "ART" and "NAT" specimens exhibited similar mineralogical composition (mainly calcite) but different grain size (coarser for the Proconnesian marble, Figure 2). Nonetheless, considering that both the "ART" and "NAT" specimens and the marble sample from the sarcophagus exhibited comparable microcracking (Figure 2), laboratory specimens were regarded as fairly representative to evaluate the consolidants ability to heal microcracks and improve marble cohesion. Moreover, the "NAT" specimens, which had undergone a similar process of biodeterioration and cleaning by the same methods, were considered in a condition similar to that of the sarcophagus, in terms of possible residues of microorganisms and/or cleaning products. Therefore, taking into account these two aspects (microcracking and former biocolonization), laboratory specimens were considered as sufficiently meaningful to evaluate the performance of the consolidants in the field.

Before cleaning   **After cleaning**   **After sawing**

Figure 3. Naturally weathered slab, before and after cleaning, and "NAT" specimens.

8

2.2. Laboratory testing

2.2.1 Consolidating treatments

The following three consolidants were tested and compared to the untreated condition (labelled as "UT").

Nanolime treatment (labelled as "NL"). The commercial product Nanorestore Plus® Ethanol 5 by CSGI (Italy) was used. It consists of a dispersion of calcium hydroxide nanoparticles in ethanol, with a concentration of 5 g/L. The product was applied by brushing (3 brush strokes) onto one 5×5 cm^2 face of the "ART" specimens and one 10×4 cm^2 face of the "NAT" specimens, waiting for the product to be absorbed between consequent brush strokes. Following the recommendation on the product's technical data sheet, the nanolime dispersion was not applied directly onto the marble surface, but a sheet of Japanese paper was interposed, to avoid white haze formation. At the end of brushing, the treated surface (still covered with the Japanese paper) was further covered with a poultice made of cellulose pulp (MH300 Phase, Italy) and deionized water in 1:4 w/w ratio. The poultice was left over the treated specimens until it dried (after about 4 days), to favor carbonation and prevent white haze formation, as recommended in the product's technical data sheet. Before testing, the specimens were left to cure in laboratory conditions (T = 21 ± 2 °C, RH = 50±5%) for 4 weeks, according to the technical data sheet.

Nanosilica treatment (labelled as "NS"). The commercial product Nano ESTEL® by CTS (Italy) was used. It consists of an aqueous dispersion of silica nanoparticles, with a dry residue of 30%. According to the suggestion in the technical data sheet and based on some preliminary screening tests, the product was diluted with deionized water to reach a dry residue of 15%. Like the "NL" treatment, the nanosilica dispersion was applied by brushing (3 brush strokes) onto one face of the "ART" and "NAT" specimens. Even though curing for 3-4 days is reported as sufficient in the product's technical data sheet, the specimens were left to cure in laboratory conditions for 4 weeks, similar to "NL" specimens.

Ammonium phosphate treatment (labelled as "DAP"). An aqueous solution containing 1 M DAP + 1 mM $CaCl_2$ was used. DAP ((NH_4)$_2$$HPO_4$) and calcium chloride ($CaCl_2$·$2H_2O$) were purchased from Sigma-Aldrich (assay > 99%). This formulation of the phosphate treatment was selected based on previous results, showing that this formulation is able to combine good consolidating and protective abilities [37,45,82]. Similar to the "NL" and "NS" treatments, the phosphate solution was applied by brushing (3 brush strokes) onto one face of the "ART" and "NAT" specimens. Moreover, considering that previous studies showed that the application method sensibly influences the outcome of the DAP treatment [43,65,83] and that poulticing resulted the most effective method in a comparative study on marble [65], application of the phosphate solution by poulticing was also tested. A poultice was prepared using cellulose pulp and the phosphate solution in 1:4 w/w ratio. The poultice was then applied onto one face of the "ART" and "NAT" specimens (similar to the case of brushing application), interposing a sheet of Japanese paper between the specimens and the poultice to avoid sticking. After application of the phosphate solution (either by brushing or poulticing), the specimens were wrapped with a plastic film to prevent evaporation and then left to cure for 24 hours in laboratory conditions. The specimens were then unwrapped (and the poultice removed, where present), then they were rinsed with deionized water and left to dry at room temperature until constant weight.

Similar to the case of "NL" and "NS" treatments, the DAP-treated specimens were tested after 4 weeks.

In summary, for both "ART" and "NAT" substrates, the following specimens were considered: untreated reference ("UT"), nanolime applied by brushing ("NL-BR"), nanosilica applied by brushing ("NS-BR"), DAP applied by brushing ("DAP-BR") and poulticing ("DAP-POUL"). For each condition, duplicate specimens were used.

2.2.2   Characterization

New phase morphology. The surface of untreated and treated specimens was observed using a field emission gun scanning electron microscope (FEG-SEM, Tescan Mira3, working distance = 10 mm, voltage = 10 kV). FEG-SEM samples were collected by chisel and made conductive by sputtering with aluminum before observation.

New phase composition. The new phase composition was determined by Fourier Transform Infrared Spectrometry (FT-IR), using a Perkin Elmer Spectrum Two spectrometer (ATR mode, 2000-400 cm^{-1} range, spectral resolution 2 cm^{-1}, 32 scans, data interval 1 cm^{-1}). FT-IR analysis was performed on powder samples, obtained from the specimen surface by scratching with a spatula.

Penetration depth. The depth of penetration of the liquid consolidants into the marble specimens was visually assessed by measuring the extension of the wet front starting from the treated surface. The measurement was carried out at the end of brushing application or after the poultice removal (in the case of the "DAP-POUL" specimens).

Efficacy. The consolidating ability was determined by measuring the increase in ultrasonic pulse velocity (_UPV_) after consolidation. The _UPV_ was taken as a reliable parameter to assess the marble increase in cohesion after consolidation, considering that several studies have shown the sensitivity of ultrasonic measurements to the presence of microcracks [84,85] and the strong correlation existing in marble between the _UPV_ and compressive and tensile strength [86]. _The UPV_ was measured by direct transmission method using a Matest instrument with 55 kHz transducers, using a rubber piece between the specimens and the transducers to improve the contact (without contaminating the specimens by using grease). To ensure that the transducers were pressed onto the specimens always using the same pressure, the measurements were carried out applying a constant force of 100 N. Thanks to the non-destructiveness of the ultrasonic measurement, the _UPV_ was determined on each sample before and after consolidation. The _UPV_ was measured in the directions perpendicular (UPV $\perp$) and parallel (UPV$_{//}$) to the plane of the slab, in the latter case averaging the values in the two orthogonal directions parallel to the plane. Both UPV $\perp$ and UPV $_{//}$ were measured by placing the transducers in the middle of the tested faces (the 5×5 cm^2 faces in the case of UPV $\perp$, two opposite 5×2 cm^2 faces in the case of UPV $_{//}$).

Chromatic compatibility. The possible alteration of the marble appearance caused by consolidation was evaluated by measuring the CIE Lab color parameters (_L*_ = black-white, _a*_ = green-red, _b*_ = blue-yellow) of untreated and treated specimens, using a NH310 colorimeter. For each specimen, the color parameters were measured in 3 different positions and the average _L*_, _a*_ and _b*_ parameters were then determined. The color

difference (ΔE^*) between untreated and treated specimens was calculated as $\Delta E^* = (\Delta L^{*2} + \Delta a^{*2} + \Delta b^{*2})^{1/2}$.

Pore size distribution. The open porosity and the pore size distribution of untreated and treated specimens were determined by mercury intrusion porosimetry (MIP), using a Porosimeter 2000 Carlo Erba with Fisons Macropore Unit 120. The MIP samples (about 1 cm³) were collected by chisel, in such a way to include the treated surface, because the greatest alterations in the pore system were expected to occur near the treated surface. A single specimen was tested for each condition, as preliminary tests on the untreated specimens exhibited fair reproducibility of results.

Water absorption. Water sorptivity and water absorption by capillarity (*WA*) were determined according to the European Standard EN 15801 [87]. Specimens were placed over a 1 cm-thick layer of filter papers, imbibed with deionized water. Water was let penetrate the specimens through the treated face and the weight increase was periodically registered. The test was stopped after 6 h, as this time was sufficient for the specimens to reach saturation.

2.3.   Field testing

2.3.1.   Initial condition

First, the whole sarcophagus surface was cleaned to remove the bioorganisms. Ecofriendly cleaning products, not dangerous for the operator nor the environment, were selected. After preliminary tests on the naturally weathered slab and small areas of the sarcophagus, the cover was cleaned by brush application of a gel containing enzymes (commercial product NasierGel by Brenta s.r.l., Italy). The gel was left to react for 30 minutes, then removed by using a toothbrush. The lower part of the sarcophagus, affected by more diffused biological growth, was cleaned by brush application of oregano and thyme essential oils (commercial product Essenzio by IBIX s.r.l., Italy, without further dilution). After 10 days, the surface treated by essential oils was washed using deionized water and a toothbrush. With the aim of removing some residual dark biopatinas, selected areas of the lower part of the sarcophagus were further subjected to micro-sandblasting (IBIX9 Trilogy 2019 instrument, IBIXART abrasive powder; pressure = 1 bar; particle composition = almandite (97-98%), ilmenite (1-2%), zircon (<0.2%), quartz (<0.5%); particle hardness = 7.5-8 Mohs; particle size = 125-250 µm; particle shape = rounded and sub-angular; distance = 30 cm; use of water for dust abatement). To make sure that micro-sandblasting would not result in abrasion of the marble surface, the progress of cleaning was periodically assessed. At the end of cleaning, surface observation by a digital microscope (Dino Lite Basic) revealed some isolated residues of microorganisms in intergranular fissures, indicating that marble surface had not been significantly eroded by micro-sandblasting.

After cleaning, the *UPV* was measured to assess the initial conservation state of the sarcophagus, before consolidation. *UPV* measurements were taken in June 2019, after a period of at least 4 days without rain to prevent moisture in the pores from altering the measurement. Similarly, all the consolidant applications and UPV measurements in the following phases of the study were carried out after an analogous period without rain. The parts of the sarcophagus investigated by UPV are illustrated in Figure 4, namely 8 areas

near the 4 vertical edges (2 areas for each edge, at 2 different heights), a cross low relief and a carved lion head on the south side. *UPV* measurements were carried out using the same instrument described in § 2.2.2 and placing the transducers in different ways, depending on the investigated part: measurements on the 8 areas near the vertical edges were performed by semi-direct transmission method (i.e. across the vertical edge); the cross low relief was tested by indirect surface method and the lion head was tested by direct transmission method (Figure 4).

Compared to laboratory conditions, where the pressure applied onto the transducers can be easily standardized, controlling the pressure applied onto the transducers in the field is much more challenging. Similar to the standard practice of ultrasonic testing of concrete structures, *UPV* measurements on the sarcophagus were carried out by manually applying an increasing pressure onto the transducers and registering the minimum travelling time, once the time had reached a plateau and had stabilized.

2.3.2. *Preliminary testing of the consolidants*

Consolidating treatments. The same consolidants already tested in the laboratory were preliminarily applied onto small areas (about 12×12 cm^2) near the vertical edges in the west side of the sarcophagus (Figure 4), all on the same day in June 2019. The same products and application methods described in § 2.2.1 were adopted. Each consolidant could be preliminarily tested only on a single area of the sarcophagus, specifically on the west side, to limit the interference with tourists visiting the adjacent Church of St. Vitale (the entrance of which is only a few meters from the east side of the sarcophagus).
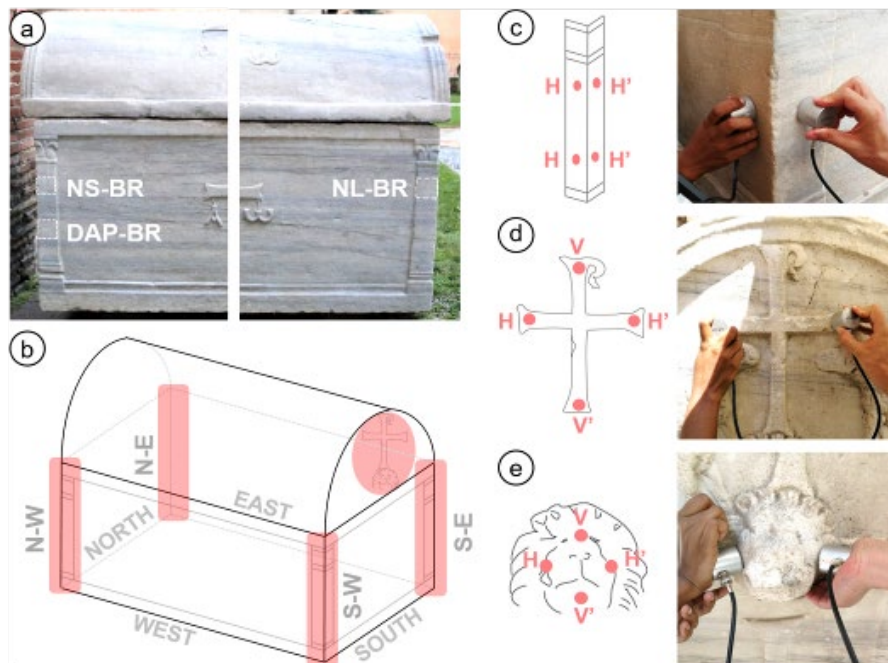
Figure 4. Field-testing on the sarcophagus: (a) indication of the areas in the west side of the sarcophagus where preliminary application of the consolidants was carried out; (b) indication of the parts analyzed by *UPV*; (c) *UPV* measurement at the four vertical edges, along the horizontal H-H' trajectory at different heights; (d) *UPV* measurement on the cross low relief, along the horizontal H-H' and the vertical V-V' trajectories; (e) *UPV* measurement across the lion head, along the horizontal H-H' and the vertical V-V' trajectories.

Unfortunately, the poultice used for the "DAP-POUL" treatment detached and fell to the ground before completion of the 24 hours of curing, therefore no conclusive results on the performance of the "DAP-POUL" treatment could be obtained by preliminary field testing.

Consolidation efficacy. To evaluate the increase in marble cohesion in the small areas treated with the various consolidants, _UPV_ measurements were repeated in October 2019 (4 months after consolidation). Possible alterations in marble appearance after consolidation were evaluated by naked eye.

2.3.3.   Final consolidation

Consolidating treatment. Putting together laboratory and field results, the "DAP-POUL" treatment was selected for consolidation of the whole sarcophagus, for the reasons discussed in § 3.2.2. The final treatment was performed in November 2019 (on different days for the cover and the lower part), following the phases illustrated in Figure S1.

Consolidation efficacy. Similar to the phase of preliminary testing, the effects of the "DAP-POUL" treatment were assessed by repeating the _UPV_ measurements in January 2020 (2 months after the final treatment). The measurements were taken in all the parts initially tested before consolidation, i.e. the 8 areas near the 4 vertical edges, the cross low relief and the lion head (Figure 4). Possible alterations in marble appearance after consolidation were evaluated by naked eye.

3. RESULTS AND DISCUSSION

3.1.   Laboratory testing

3.1.1   New phase morphology and composition

The surface morphology of untreated and treated specimens is illustrated in Figure 5, while the corresponding FT-IR spectra are reported in Figure 6.

In the "UT" condition, the "NAT" samples exhibited visible surface etching (parallel grooves over the calcite surface) and presence of extraneous compounds (small acicular elements), which were not present in the "ART" samples, as expected. In both cases, calcite was the only phase detected by FT-IR, as indicated by bands at 1397-1404 cm^{-1} (CO_3^{2-} asymmetric stretching [88]), 872-873 cm^{-1} (CO_3^{2-} out-of-plane bending [88]) and 712 cm^{-1} (CO_3^{2-} in-plane bending [88]).

After treatment with nanolimes, new crystals with distinguishable morphology were observed on the "ART-NL-BR" sample. The needle-like morphology of these crystals suggests formation of aragonite [89], a polymorph of calcium carbonate. The fact that carbonation of nanolimes may lead to formation of metastable vaterite and aragonite, rather than thermodynamically stable calcite, has been pointed out in the literature [2]. This originates from the partial conversion of nanoparticles of calcium hydroxide dispersed in alcohols into calcium alkoxides [8]. During curing in humid environment, the alcohol adsorbed onto the nanoparticles is released in the aqueous film formed on the particle surface [90]. This leads to formation of a hydroalcoholic solution on the nanoparticle

surface during carbonation, which favors the nucleation and the kinetic stabilization of vaterite and aragonite [90]. The fact that micrometric but isolated crystals of aragonite were detected in the "ART-NL-BR" samples is thought to be a consequence of the phase evolution occurring over time: while vaterite (likely formed together with aragonite) fully converts into calcite, aragonite crystals may undergo Ostwald ripening, resulting in large but scarce prisms [90]. The FT-IR spectrum of the "ART-NL-BR" sample detected only bands owing to calcite, either coming from the substrate or originated from vaterite transformation. No band owing to aragonite (having bands at 1489, 856, 714 and 700 cm^{-1} [88], hence distinguishable from calcite) was detected. This is likely a consequence of the very low amount of aragonite, present in large but isolated crystals as discussed above. In the case of the "NAT-NL-BR" sample, similar considerations can be made. New crystals were visible on the marble surface, even though fewer crystals with morphology ascribable to aragonite were present. Similar to the case of the "ART" sample, also in the "NAT" sample only calcite was detected by FT-IR.
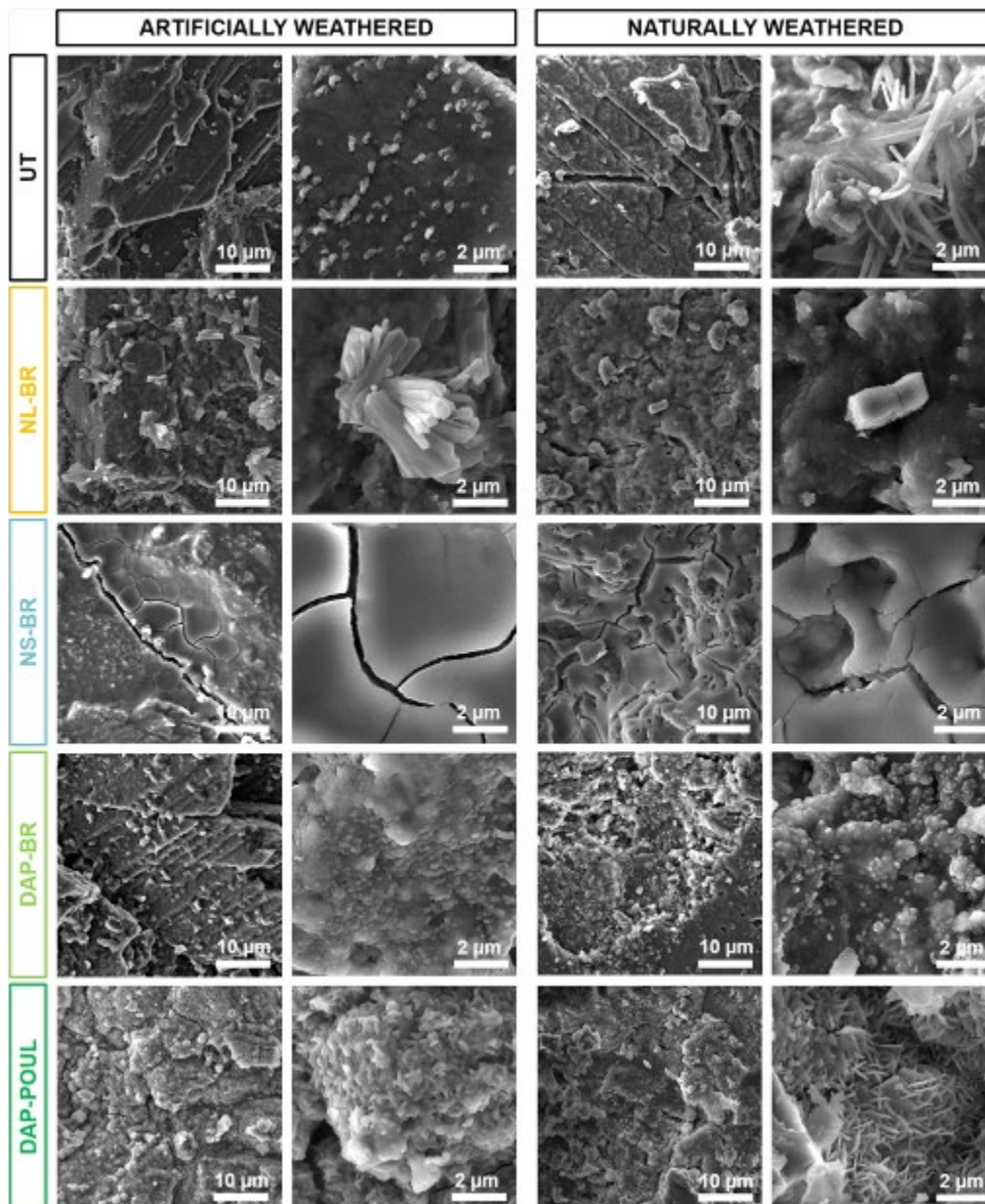
Figure 5. Surface morphology of untreated and treated specimens of artificially and naturally weathered marble.
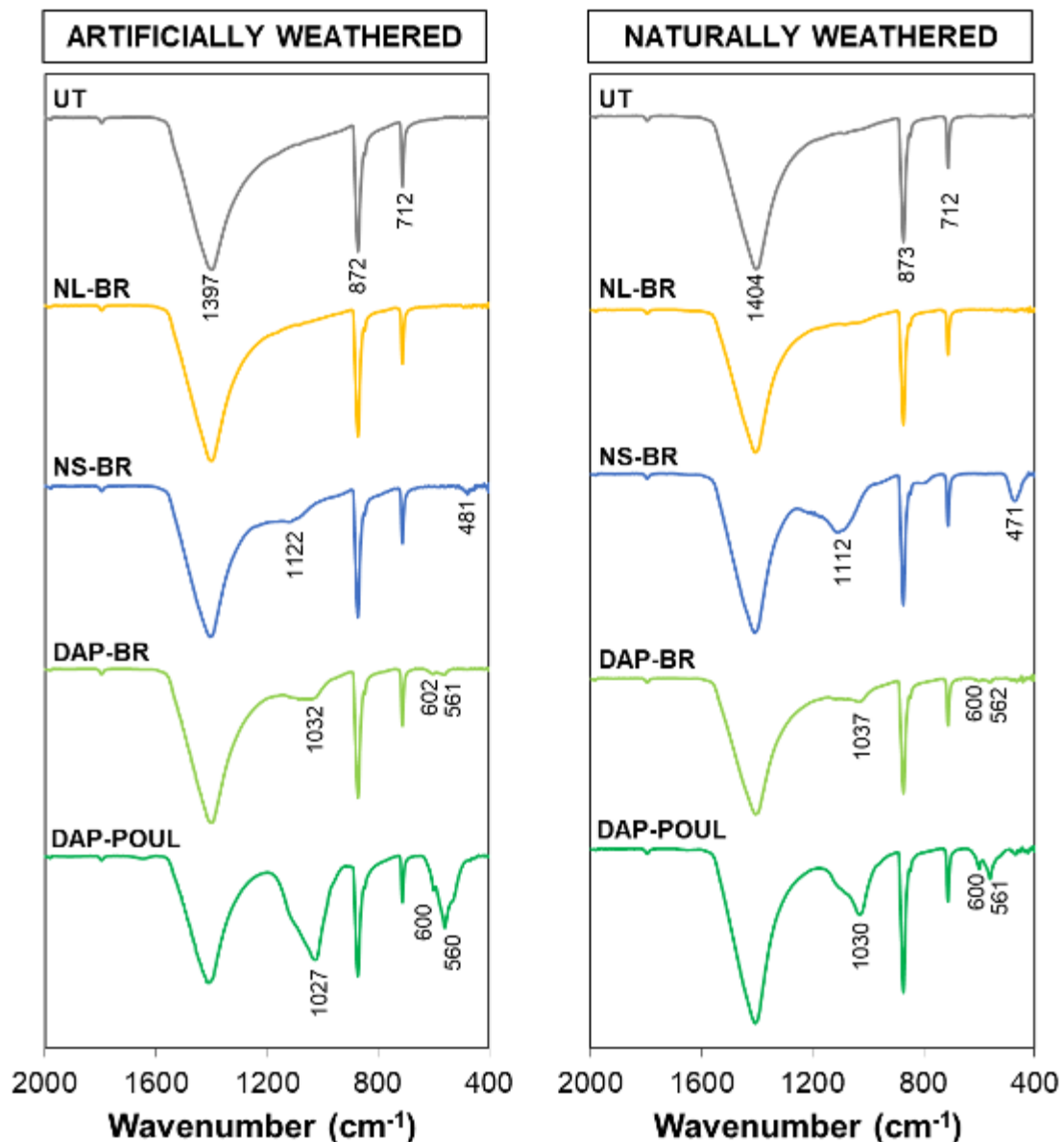
Figure 6. FT-IR spectra of untreated and treated specimens of artificially and naturally weathered marble (the position of bands owing to calcite is reported in the untreated reference and omitted in the treated samples for a better readability).

After treatment with nanosilica, a surface crust, affected by diffused cracking, was clearly visible both in the "ART" and in the "NAT" samples. Nanosilica accumulation on the treated surface, with formation of a thick crust, was reported in the literature also in the case of other stone types [9,12], even with high porosity [9], hence it is not limited to the case of marble. As expected, FT-IR spectra of both the "ART" and "NAT" samples exhibited bands owing to silica (bands at 1112-1122 cm^{-1} owing to Si-O-Si symmetric stretching [91] and 471-481 cm^{-1} owing to O-Si-O bending [91]), alongside bands owing to the calcitic substrate. Comparing the "ART" and the "NAT" samples, the higher intensity of the FT-IR bands and the more diffused cracking observed in the latter sample may suggest formation of a thicker surface layer over the "NAT" sample, which is consistent with its lower porosity (see § 3.1.4). However, further tests would be needed to verify this hypothesis.

15

After treatment with the DAP solution applied by brushing, in both the "ART-DAP-BR" and the "NAT-DAP-BR" samples the morphology of the underlying marble surface was still visible. However, observation at high magnification revealed that the marble surface had reacted with formation of a continuous layer of small new crystals. Formation of similar crystallites after treatment with DAP solutions has been reported in previous studies [30,92]. In the FT-IR spectra, these new crystals gave rise to new bands at 1032-1037 cm^{-1}, 600-602 cm^{-1} and 561-562 cm^{-1}. These new bands can be attributed to HAP, having bands at 1031-1032 cm^{-1} (PO_4^{3-} antisymmetric stretching [88,93]), 602-604 cm^{-1} and 561-563 cm^{-1} (PO_4^{3-} antisymmetric bending [88,93]). The possible formation of OCP, having bands at 1023-1026 cm^{-1}, 1036-1038 cm^{-1}, 602-603 cm^{-1} and 560 cm^{-1} [88,93], seems excluded because two distinct bands should be present at 1023-1026 cm^{-1} and 1036-1038 cm^{-1}. However, for a conclusive identification further analyses would be necessary.

In the case of DAP application by poulticing, the marble surface of both the "ART-DAP-POUL" and "NAT-DAP-POUL" samples was covered with new phases with characteristic features. Whereas brushing application led to formation of a surface coating made of small crystallites, poultice application promoted formation of elongated crystals with the typical flower-like morphology of HAP [37,42,64]. The presence of cracks in the layer formed after treatment by poultice is likely a sign that a thicker film was formed, compared to brushing application. In fact, cracking is originated by stress that arises during drying: when the layer thickness is below a certain critical value, cracking is thermodynamically unfavored, while cracking occurs when the layer thickness exceeds this critical value [94]. Consistently, in a previous study on DAP treatment of a porous limestone a thicker surface film (~5-10 μm thickness) was found after treatment by poultice, compared to treatment by brushing (~1-2 μm thickness) [83]. However, specific analyses would be needed to ascertain the film thickness in the present case. FT-IR results suggest more abundant formation of new CaP phases in the case of poultice application, compared to brushing, as the new bands in the "DAP-POUL" samples were much more pronounced compared to the "DAP-BR" ones. The new bands in the "DAP-POUL" samples appeared at 1027-1031 cm^{-1}, 600 cm^{-1} and 560-561 cm^{-1}, which also in this case can be attributed to formation of HAP [88,93]. In general, more abundant formation of new consolidating phases in case of DAP application by poulticing, compared to brushing, is consistent with previous results obtained on limestone [43] and marble [65].

Notably, in the case of the "ART-DAP-POUL" sample (but not in the "NAT" companion), SEM observation also detected acicular plate-like crystals, formed over the HAP layer in some isolated areas (Figure 7). The morphology of these acicular crystals suggests formation of brushite, which was confirmed by FT-IR analysis. In these areas, new bands at 1068 cm^{-1} (with a shoulder at 1131 cm^{-1}) and 559 cm^{-1} (with a shoulder at 532 cm^{-1}) were found, which are compatible with formation of brushite, having bands at 1063-1064 cm^{-1} and 1130-1136 cm^{-1} (PO_4^{3-} antisymmetric stretching), 576-577 cm^{-1} and 525-528 cm^{-1} (PO_4^{3-} antisymmetric bending [88,93]). Brushite formation over a layer of HAP (mixed with OCP) has been previously reported in the literature, in the case of marble treated with various DAP solutions [42]. Formation of brushite ($CaHPO_4 \cdot 2H_2O$) was explained considering that it requires: (i) fewer Ca^{2+} ions compared to HAP (the Ca/P ratio being 1 for brushite and 1.67 for HAP) [42]; (ii) HPO_4^{2-} ions, while HAP requires PO_4^{3-} ions [42]; (iii) low pH, while HAP formation is favored at high pH [39]. These conditions favorable to brushite precipitation occur at the end of the DAP treatment, when Ca^{2+} and PO_4^{3-} ions in

the starting DAP solution are progressively consumed to form HAP, with a consequent pH decrease [42]. As a result, brushite precipitates *over* the already-formed HAP layer. In any case, this is not expected to affect negatively the consolidating ability of the "DAP-POUL" treatment. In fact, even if brushite is washed away by rain (being soluble at pH>4 [39]), the underlying HAP layer will continue to exert its preservation action on marble.

Based on the obtained results, no interference seems to have occurred between the consolidating treatments and possible residues of bioorganisms and/or cleaning products that might have remained in the "NAT" specimens (although no such residue has been experimentally identified). In fact, no unexpected reaction product was detected in the "NAT" samples. However, to conclusively ascertain that no interference occurred even in some isolated part, additional analyses would be needed.
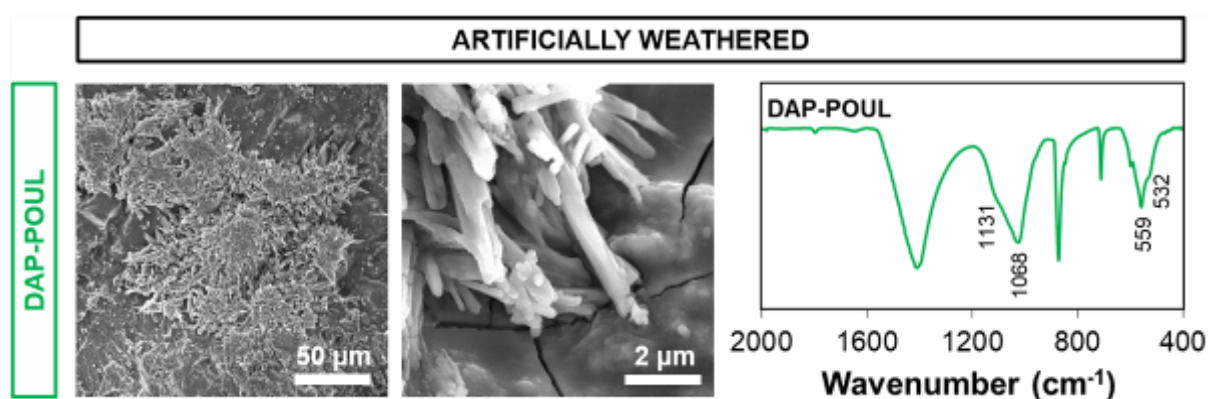
Figure 7. Morphology and FT-IR spectrum of brushite precipitated over HAP in artificially weathered marble.

### 3.1.2   *Penetration depth and effectiveness*

The depth of penetration of the liquid consolidants into artificially and naturally weathered specimens is illustrated in Figure 8. In general, the penetration depth was higher in the "ART" specimens (2.5 to 8 mm) than in the "NAT" ones (2 to 3.5 mm), which is consistent with the higher porosity and higher sorptivity of the "ART" specimens (cf. § 3.1.4). On either type of substrate, the highest penetration depth was registered for the DAP solution, reaching 8 mm when applied by poulticing on the "ART" specimens and 3.5 mm when applied by brushing on the "NAT" ones. In both types of substrate, the nanolime suspension exhibited the lowest penetration depth (2 mm in the "NAT" specimens, 2.5 mm in the "ART" ones). The nanosilica dispersion exhibited a deeper penetration in the "ART" specimens (down to 5 mm), compared to the "NAT" ones (limited to 2 mm). In the case of the "ART" substrate, having higher porosity than the "NAT" one, the penetration depth of nanosilica was likely helped by the very small size of the nanoparticle (10-20 nm, according to the product's technical data sheet). In the case of the "NAT" substrate, the low porosity and the low sorptivity are thought to be the limiting factors responsible for the scarce penetration depth of both nanoconsolidants.
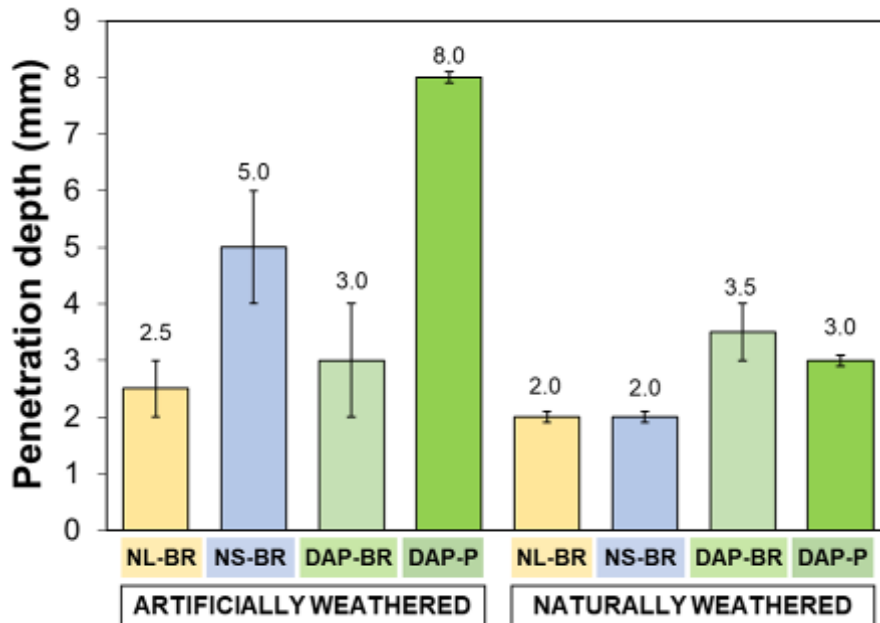
Figure 8. Penetration depth of the consolidants into artificially and naturally weathered specimens (values are averages for 2 specimens, bars indicate the difference between the average and the maximum/minimum values).

When evaluating the penetration depth of a consolidant based on the depth of the wet fringe registered right at the end of the consolidant application, several aspects should be considered. First, the wet fringe indicates the presence of the solvent but not necessarily of the nanoparticles (NL and NS treatments) or the ions (DAP treatment) originally dispersed or dissolved in the solvent. In fact, phase separation between the nanoparticles and the solvent or chemical reaction between the ions and the substrate might have occurred. Second, liquid consolidants are known to be progressively absorbed into finer pores, where absorption is slower [21]. For this reason, previous studies pointed out an increase in penetration depth of the DAP solution after the end of the solution application [49,95]. Finally, during drying liquid consolidants are transported back towards the surface where evaporation takes place, which has been found to cause accumulation of nanolimes [4] and more abundant formation of HAP [95] near the treated surface.

In any case, the trends in penetration depth illustrated in Figure 8 offer useful information to understand the different consolidating abilities of the various treatments, reported in Figure 9. The consolidating ability was evaluated in terms of ultrasonic pulse velocity (*UPV*), which has been historically used to evaluate the conservation state of marble, based on the damage classification proposed by Köhler [96]. An adaption of this classification is illustrated in the upper graph in Figure 9. According to this damage classification, the conservation state of marble can be distinguished in 5 different classes, ranging from the "fresh" condition (*UPV* > 5 km/s) to the "disintegrated" condition (*UPV* < 1.5 km/s) [96].
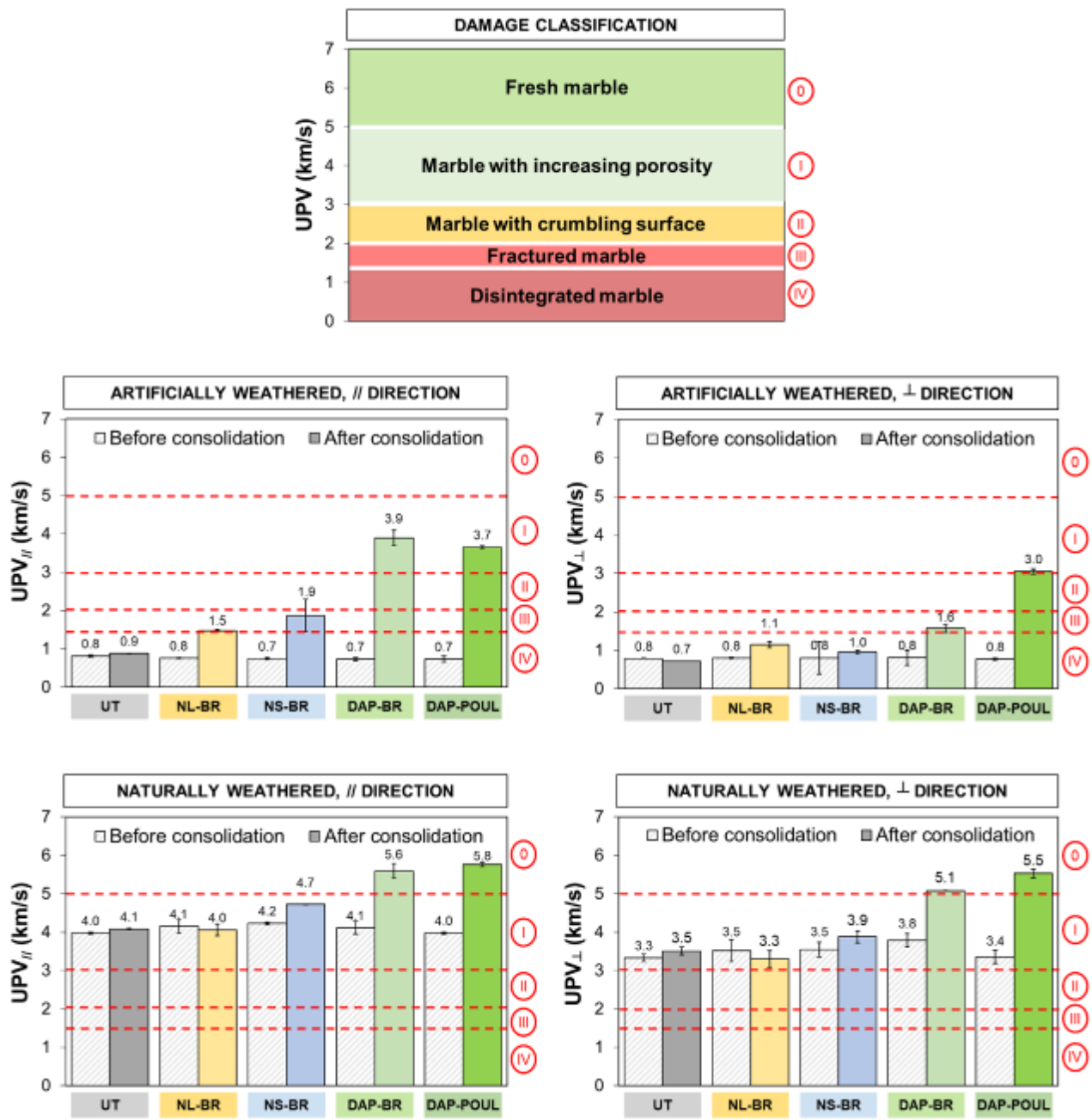
Figure 9. Ultrasonic pulse velocity (*UPV*) of artificially and naturally weathered specimens, before (dashed bars) and after (solid bars) consolidation (values are averages for 2 specimens, bars indicate the difference between the average and the maximum/minimum values). In the upper graph, an adaptation of the damage classification proposed by Köhler [96] is shown.

In the case of the "ART" substrate, before consolidation all the specimens exhibited *UPV* = 0.7-0-8 km/s, thus belonging to the "disintegrated marble" category. This is a result of artificial weathering performed by heating at 400 °C (cf. § 2.1.2). After consolidation and curing, when the *UPV* of the consolidated specimens was re-measured, also the untreated references were re-tested, to ensure the repeatability of the measurement. Only minor variations were registered (~0.1 km/s), which can be ascribed to the experimental error of the technique, so the reliability of the *UPV* results was confirmed.

After treatment by nanolimes, minor increases in *UPV* were registered both parallel and perpendicular to the plane of the small slabs, so that no significant improvement from the "disintegrated marble" condition was experienced. Different reasons may exist for the limited mechanical improvement, namely the scarce penetration depth of the nanolime dispersion (Figure 8) and the formation of metastable calcium carbonate phases after carbonation [2]. In fact, previous studies have shown that the full consolidation capacity of nanolimes is not reached until full conversion of metastable calcium carbonate phases into stable calcite is achieved, which may take several months [2]. In the present case, considering that only isolated aragonite crystals were detected, with no vaterite crystals (likely fully converted into calcite), the scarce consolidating ability seems to be mainly ascribable to the low penetration depth of the nanolime dispersion.

In the case of nanosilica, *UPV* increased from 0.7 to 1.9 km/s in the parallel direction, while it only increased from 0.8 to 1 km/s in the perpendicular one. This difference in consolidating ability between the two directions can be explained considering the penetration depth of the nanosilica dispersion, which reached 5 mm out of 20 mm of total thickness of the "ART" specimens (Figure 8). In the parallel direction, these 5 mm of consolidated marble are sufficient to improve the *UPV* from 0.7 to 1.9 km/s, as the ultrasonic pulse travels through the densest layer available (even though this layer has a thickness of only 5 mm out of 20 mm). Differently, in the perpendicular direction the ultrasonic pulse has to cross the unconsolidated layer and, being 15 mm out of 20 mm, this unconsolidtaed layer significantly reduces the crossing time. Even in the parallel direction, the *UPV* exhibited a limited increase (not exceeding the "fractured marble" condition), likely because of the lack of chemical bonding between the substrate and the consolidant. In fact, given the lack of OH⁻ groups on the calcite surface, which may allow for chemical bonding, only deposition of silica in the intergranular fissures and some improvement in cohesion may take place [33]. However, no significant improvement in mechanical properties can be expected from this type of consolidant when applied onto carbonate stones, similar to the case of ethyl silicate [21]. The encouraging increases in mechanical properties reported for carbonate stones treated with nanosilica dispersions [22,24] are probably to be ascribed to the presence of some quarzitic fractions in the investigated lithotypes [22].

In the case of the DAP solution applied by either method, the penetration depth had a similar influence as discussed above for nanosilica. In the parallel direction, "DAP-BR" and "DAP-POUL" specimens underwent similar increases in *UPV* (from 0.7 up to 3.9 and 3.7 km/s, respectively), because the ultrasonic pulse travels through the consolidated layer (even though the thickness of this layer is different in the two cases). In the perpendicular direction, the "DAP-POUL" specimen exhibited an *UPV* increase (up to 3.0 km/s) much higher than that of the "DAP-BR" specimen (up to 1.6 km/s), because the penetration depth in the "DAP-POUL" specimen (8 mm) is much higher than in the "DAP-BR" specimen (3 mm). As a result, the influence of the unconsolidated layer, which the ultrasonic pulse has to cross in the perpendicular direction, is lower in the "DAP-POUL" specimen. For both application methods, it is very likely that the final depth of formation of the new consolidating phases was actually higher than assessed right at the end of brush or poultice application [29,43,95], so the influence of the unconsolidated layer might have been further reduced. Notably, consolidation by DAP was the only treatment able to improve marble conservation state so as to reach the "increasing porosity" condition,

which is the lowest damage class after the "fresh marble" condition (Figure 9). Such improvement was possible because the consolidating effect of the DAP treatment is not due to mere occlusion of intergranular fissures (like in the case of nanosilica), but is due to formation of new phases that are chemically bonded to the calcite grains and able to effectively bridge them. This was demonstrated in previous studies where, together increases in *UPV*, DAP-treated marble showed significant increases in resistance to abrasion [29], resistance to material loss by peeling [29] and resistance to thermal weathering [30].

In the case of the "NAT" substrate, before consolidation specimens exhibited a less dramatic deterioration state than the "ART" specimens, as they belonged to the category of "marble with increasing porosity" (Figure 9). It is noteworthy that, unlike the "ART" ones, all the untreated "NAT" specimens exhibited lower *UPV* in the perpendicular direction (3.3 to 3.9 km/s) than in the parallel one (4.0 to 4.2 km/s). Similar to the influence of penetration depth, the difference in *UPV* measured in the perpendicular and parallel directions suggests a gradient in marble cohesion across the specimen thickness. This is likely a consequence of the biodeterioration that initially affected the naturally weathered marble and that was removed by cleaning before consolidant application (cf. § 2.1.2).

Treatment by nanolimes led to basically no improvement in *UPV* in either direction, for the same reasons discussed in the case of the "ART" specimens, mostly the scarce penetration depth.

Consolidation by nanosilica, which exhibited limited penetration depth as well, increased *UPV* in both directions to some extent, because of some silica deposition in the intergranular fissures. However, the increase in cohesion was limited, so that marble remained in the "increasing porosity" category, for the same reasons discussed in the case of the "ART" specimens.

Consolidation by DAP, applied by either brushing or poulticing, was the only treatment able to significantly improve marble condition, so as to reach the "fresh" condition. The two application methods exhibited similar penetration depth and gave similar *UPV* increases in both directions, the "DAP-POUL" treatment always causing the greatest improvement.

In summary, both in the artificially and naturally weathered specimens, the treatments exhibited a consolidating ability decreasing in the following order: DAP-POUL > DAP-BR >> NS-BR ≈ NL-BR ≈ UT. This trend is a consequence of both the different ability of the various consolidants to penetrate deeply into the substrate and the different capacity to chemically bond to it and bridge the calcite grains.

3.1.3   *Chromatic compatibility*

The color parameters of untreated and treated "ART" specimens are reported in Table 1, while the resulting color difference (ΔE^*) is illustrated in Figure 10.

In the "ART" specimens, all the treatments caused some slight darkening (decrease in L^*). Nanosilica was the only treatment responsible for a shift towards green (decrease in a^*) and blue (decrease in b^*), while all the other consolidants caused shifts towards red (increase in a^*) and yellow (increase in b^*). In the case of nanosilica and DAP applied by poulticing, the resulting color difference was higher than the threshold of visibility by the

human eye ($\Delta E^* = 2.3$ [97]). Nonetheless, for all treatments the color difference was lower than the threshold commonly accepted for conservation treatments ($\Delta E^* = 5$ [98]).

In the case of the "NAT" specimens, visible color differences were present even before treatment (Figure 3), as a result of the different initial conditions and different cleaning methods applied in the various parts of the slab. Unfortunately, it was not possible to measure the color parameters of each specimen before and after consolidation, but the color difference could only be evaluated between untreated and treated specimens. However, evaluating the aesthetic effects of the consolidants by comparing specimens that originally had clearly visible differences would be scarcely significant. Therefore, the evaluation of the aesthetic compatibility of the treatments was based only on the results obtained on the "ART" specimens, which indicate that all the treatments can be considered as fairly compatible.

Table 1. Color parameters (L^* = black-white, a^* = green-red, b^* = blue-yellow) of untreated and treated artificially weathered specimens (values are averages for 3 measurements).

"ART" specimens	L^*	a^*	b^*
UT	91.5	-0.5	2.8
NL-BR	90.4	-0.7	2.5
NS-BR	88.2	-0.2	3.2
DAP-BR	90.1	-1.0	1.2
DAP-POUL	89.5	-0.8	1.4
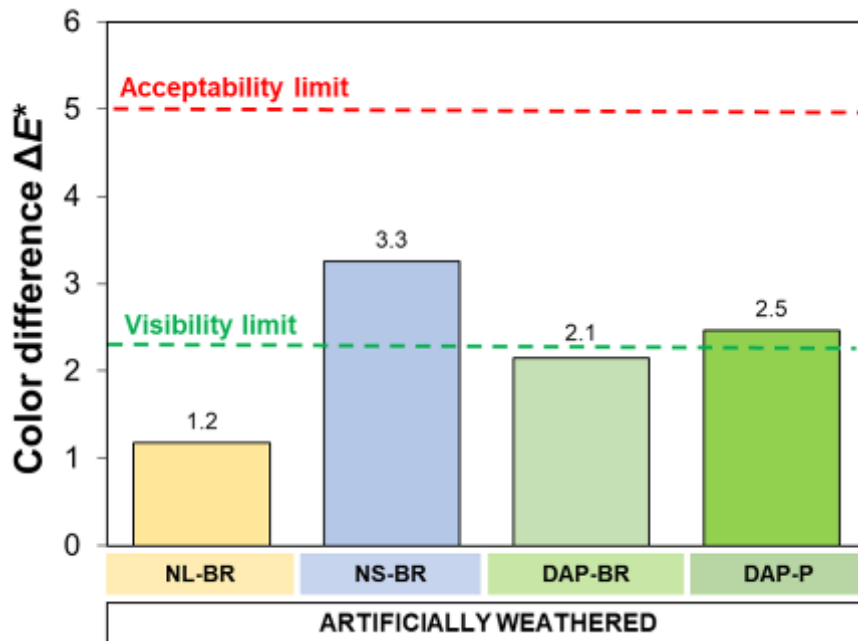
Figure 10. Color difference (ΔE^*) between untreated and treated specimens of artificially weathered marble.

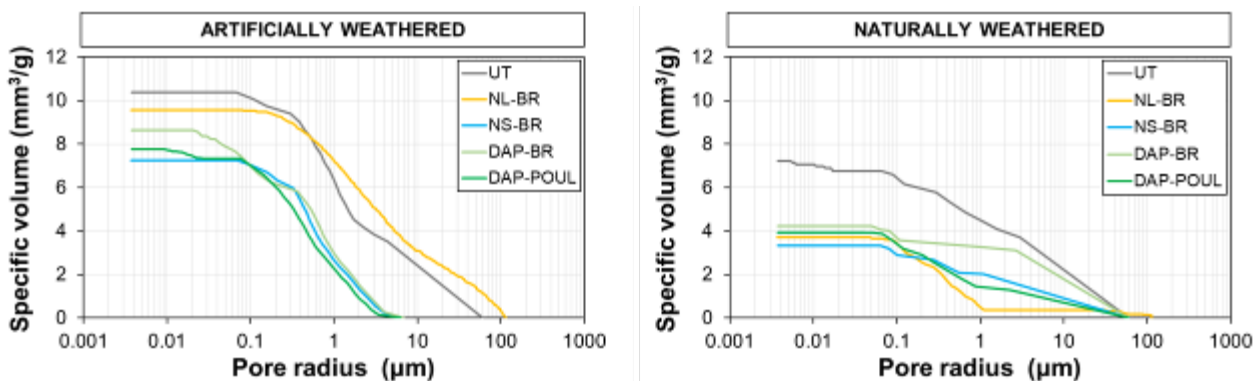### 3.1.4   Pore size distribution and water absorption

The pore size distribution of untreated and treated samples of artificially and naturally weathered marble are illustrated in Figure 11. In the untreated condition, the "ART" substrate exhibited higher open porosity than the "NAT" one (2.9% and 2.1%, respectively).

In the "ART" samples, consolidation by nanolimes caused the lowest alteration in the pore system (open porosity only decreasing to 2.4%), consistently with the limited penetration depth of this treatment (Figure 8). The other consolidants caused slightly more pronounced alterations in the pore size distribution, especially in the amount of coarse pores. The resulting open porosity ranged between 1.9 and 2.4%, but in no case did complete pore occlusion take place, consistently with previous results [29,30].

In the case of the "NAT" specimens, all treatments caused some reduction in open porosity, from 2.1 to 1.0-1.2%. Compared to the "ART" specimens, the main difference was the effect of the "NL-BR" treatment, which apparently caused the greatest change in the pore system. However, as discussed above, when evaluating results on the "NAT" specimens it should be borne in mind that these specimens had slightly different initial conditions, because they were obtained from parts of the naturally weathered slab initially affected by different biological deterioration and cleaned by different methods.

As a consequence of these alterations in the pore system, the changes in water sorptivity reported in Figure 12 were registered. Both the artificially and naturally weathered substrates exhibited quite low water absorption (*WA*), reaching 0.8 wt% for "ART" and 0.2 wt% for "NAT" specimens.

In the "ART" specimens, nanolimes, nanosilica and DAP applied by brushing caused a similar reduction in water sorptivity, while DAP applied by poultice was responsible for a more pronounced alteration. The reduction in sorptivity registered for the "DAP-POUL" specimen is owing to the greater alteration in the pore system induced by poulticing compared to brushing, as pointed out also in previous studies [43]. However, in spite of the initially slower absorption rate, the final *WA* of the "DAP-POUL" specimen was fully comparable to that of the other treatments.

Figure 11. Pore size distribution of untreated and treated samples of artificially and weathered marble.
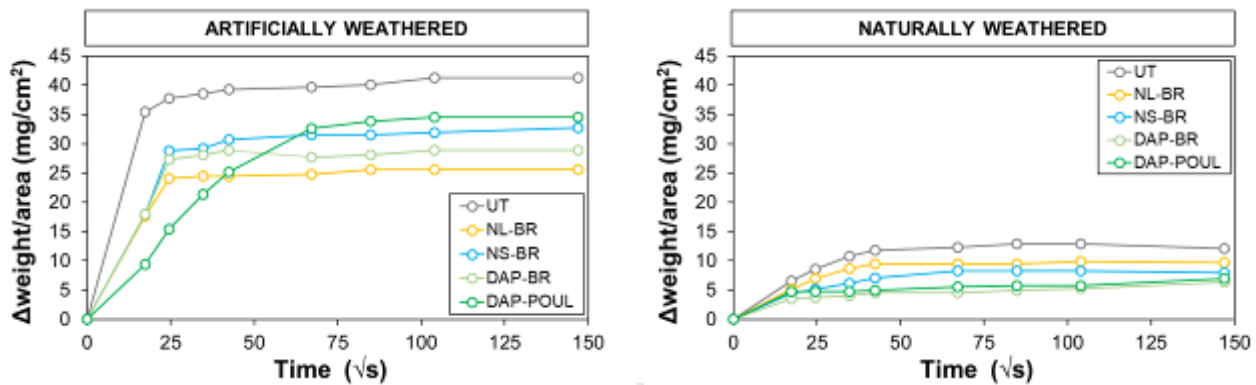
Figure 12. Water sorptivity of untreated and untreated samples of artificially and weathered marble.

In the case of the "NAT" specimens, all the treatments were responsible for some decrease in the water sorptivity and in the final *WA*, which however was very low even in the untreated reference.

In summary, none of the consolidating treatments was responsible for complete pore occlusion and for dramatic alterations in the water sorption behavior. Therefore, they can all be considered as compatible from a physical-microstructural point of view.

3.2. Field-testing

3.2.1 Initial condition

The *UPV* values registered before consolidation in the different parts of the sarcophagus are reported in Figure 13 (dashed bars). Depending on the exposure, different conservation conditions were assessed in the different parts of the sarcophagus.

The west side (where preliminary field-testing was carried out) actually exhibited high *UPV* values (ranging from 5.5 to 6.9 km/s), corresponding to the "fresh marble" condition. In the east side, lower *UPV* values were registered, ranging from 4.3 to 5.3 km/s, hence close to the threshold of 5 km/s separating the "fresh marble" and the "marble with increasing porosity" conditions. In the south side, the lowest *UPV* values were registered (*UPV* ranging from 2.7 to 4.3 km/s), which is consistent with the greater solar radiation received by architectural elements facing south. The cross low relief exhibited *UPV* values of 2.7-2.8 km/s, indicating "marble with crumbling surface". Such low *UPV* values can be explained considering that small carved elements are known to undergo more pronounced thermal weathering, as they follow temperature variations more closely than large massive elements [28]. Moreover, it should be noted that the cross low relief was tested by indirect surface method, which is strongly influenced by the damage condition of the most superficial layer of the tested element, although it is difficult to quantify the thickness of this layer. The lion head, tested by direct transmission method, gave *UPV* values of 4.1 to 4.3 km/s, corresponding to the condition of "marble with increasing porosity".
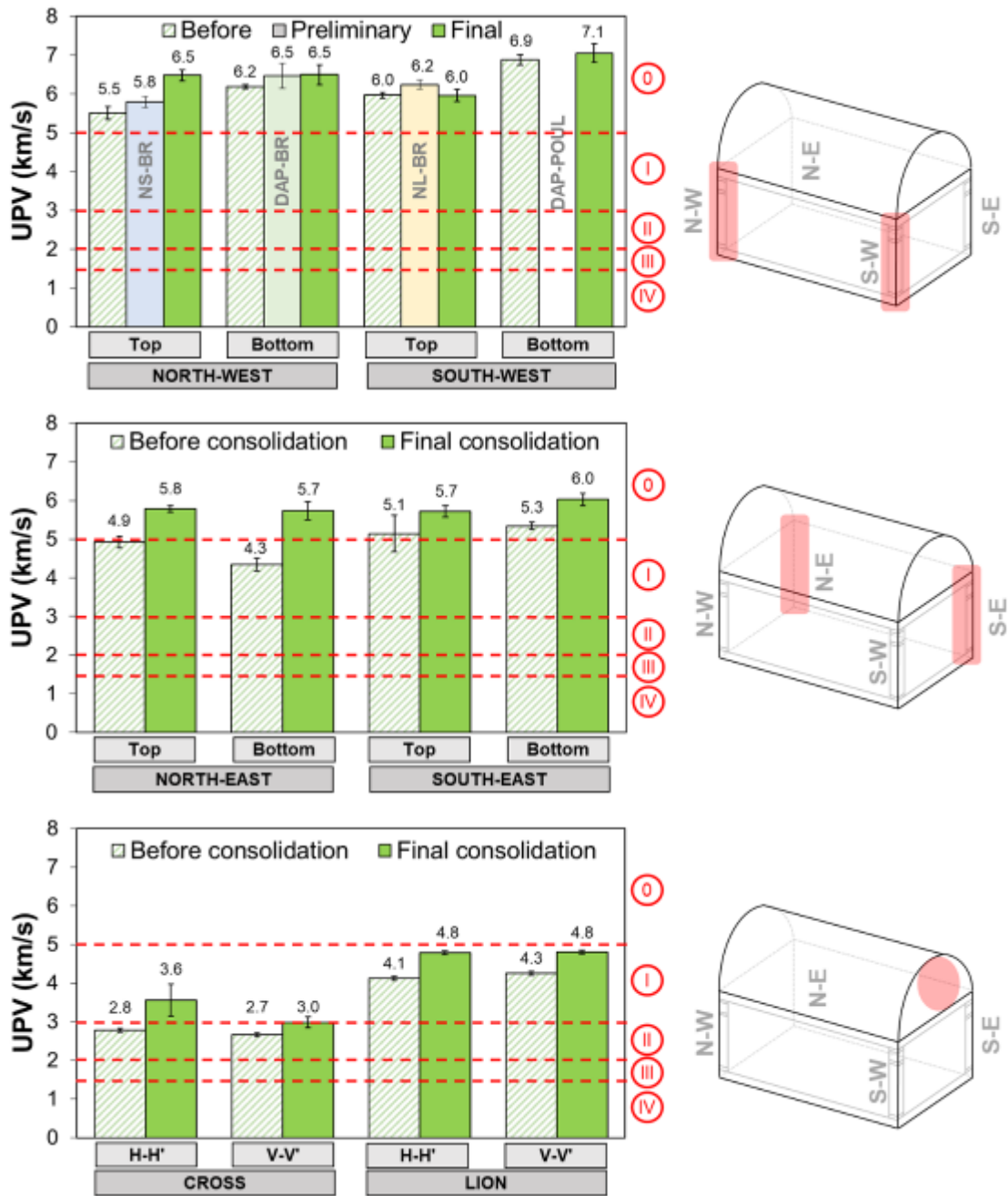
Figure 13. *UPV* of various parts of the sarcophagus (values are averages for 3 measurements, bars indicate the difference between the average and the maximum/minimum values): before consolidation (dashed bars); after preliminary consolidation by the various treatments (intermediate bars in the upper graph); after final consolidation by the "DAP-POUL" treatment (dark green bars).

3.2.2   Preliminary testing of the consolidants

The consolidating treatments were applied on small areas of the sarcophagus (cf. § 2.3.1), to evaluate the treatment performance in real conditions. The *UPV* increases in the tested areas are reported in the upper graph in Figure 13.

Nanolimes, nanosilica and DAP applied by brush all caused some increases in *UPV*, but in all cases the improvements were actually quite modest (maximum Δ*UPV* = 0.3 km/s). While nanolimes and nanosilica exhibited modest consolidating ability also in the

laboratory, for the "DAP-BR" treatment the *UPV* increase measured in the field (ΔUPV = 0.3 km/s) is lower than that assessed on the laboratory specimens (ΔUPV = 0.8-3.2 km/s). This can be explained considering that the west side of the sarcophagus, selected for preliminary testing for the reasons described in § 2.3.2, actually exhibited a good conservation state ("fresh marble"), definitely better than other parts of the sarcophagus ("marble with crumbling surface"). As pointed out in previous studies, the higher the substrate deterioration, the higher the consolidating action of a consolidant [35]. Therefore, the modest consolidating efficacy of the "DAP-BR" treatment may be ascribed to the initial good conservation state of the tested area.

In the case of the DAP treatment applied by poultice, as mentioned in § 2.3.1 the poultice unfortunately detached and fell to the ground before completion of the 24 hours of curing, hence no data on the consolidating effectiveness of this treatment could be obtained from preliminary field-testing.

In terms of aesthetic compatibility, none of the consolidants caused dramatic alterations of the marble surface, as illustrated in Figure S2.

All things considered, preliminary field testing confirmed the aesthetic compatibility of all the treatments, but also exhibited some limitation in the capability to reliably evaluate the consolidating action of the treatments. In fact, the deterioration condition of the laboratory specimens allowed to highlight the different abilities of the various consolidants to penetrate in depth and increase marble cohesion; on the contrary, the good conservation state of the west side of the sarcophagus, where preliminary testing was performed, substantially flattened the performance of the various consolidants. For this reason, laboratory results seem more significant and more reliable to evaluate the potential of the various treatments. Considering that in laboratory conditions the "DAP-POUL" treatment stood out as the most promising consolidant, able to combine high efficacy and compatibility on both the "ART" and the "NAT" specimens, this treatment was selected for application onto the whole sarcophagus, as described in § 2.3.2.

3.2.3   Final consolidation

After consolidation by the "DAP-POUL" treatment, the *UPV* values measured in all the parts of the sarcophagus characterized before consolidation (i.e. the four edges, at two different heights, the cross low relief and the lion head) are illustrated in Figure 13 (dark green bars). In general, the "DAP-POUL" treatment caused significant *UPV* increases, the improvement varying as a function of the initial weathering condition.

In the west side, where marble was initially in a better conservation state than the other parts of the sarcophagus, the lowest *UPV* increases were registered (ΔUPV = 0 to 1 km/s). In the east side, where in some areas marble was in the "increasing porosity" condition, higher improvements were found, reaching ΔUPV = 1.4 km/s in the most damaged part. After consolidation, all the investigated areas in the east side reached the "fresh marble" condition. In the south side, the carved elements that initially exhibited the lowest *UPV* values underwent improvements up to ΔUPV = 0.8 km/s. In this way, even the most damaged area (the cross low relief) improved its condition from "crumbling surface" to "increasing porosity".

The above described increases in cohesion were reached without significant alteration of the marble surface (such as white hazes or surface staining), as illustrated in Figure S3.

4. CONCLUSIONS

The present study was aimed at comparing commercial dispersions of nanolime and nanosilica with an aqueous solution of diammonium phosphate as possible consolidating treatments for marble. The comparison was carried out both in laboratory (on samples showing different levels and types of deterioration) and in the field (on a byzantine marble sarcophagus). The obtained results allow to derive the following conclusions:

1) In laboratory conditions, the treatment based on ammonium phosphate outperformed commercial nanolime and nanosilica. In fact, the nanolime dispersion exhibited limited penetration depth and, consequently, very low consolidating capacity. The nanosilica dispersion showed limited penetration as well, which, combined to the lack of chemical bonding to the substrate, led to low consolidation. Notably, the ammonium phosphate treatment exhibited higher penetration depth and higher consolidating effectiveness than both nanoconsolidants, especially when applied by poulticing. All the treatments proved to be sufficiently compatible from the aesthetical point of view and in terms of alterations in the pore system and water transport properties. In addition to the higher effectiveness, the ammonium phosphate treatment also has the advantage of being effective after just 24 hours, whereas curing for a few days is necessary for nanosilica and for more than one month in the case of nanolimes.

2) When tested on a byzantine marble sarcophagus, nanolimes, nanosilica and ammonium phosphate applied by brush caused minor alterations in the appearance of the marble surface, but also modest increases in marble cohesion assessed by ultrasounds. The lack of substantial mechanical improvement was mostly due to the relatively good conservation state of marble in the tested areas. Considering that laboratory testing on weathered specimens allowed to highlight the different abilities of the various consolidants to penetrate in depth and increase marble cohesion, while field testing on the scarcely deteriorated side of the sarcophagus flattened the performance of the various consolidants, laboratory results were considered as more significant. Consequently, ammonium phosphate applied by poulticing was regarded as the most promising treatment and selected for consolidation of the whole sarcophagus. After consolidation by this treatment, significant increases in marble cohesion were registered, especially in the most deteriorated parts (i.e. small carved elements, where thermal weathering was most pronounced). After consolidation, no significant alteration of the marble appearance was visible by naked eye.

By highlighting the pros and the cons of the investigated consolidants, this study aims to provide practitioners with objective data to guide the selection of the most suitable product for consolidation of marble artworks. The high potential of the ammonium phosphate treatment was confirmed, both in laboratory and in the case study, which is expected to contribute to the further diffusion of this treatment in the practice of monument conservation. Continue monitoring of the sarcophagus in the future will help systematically assess the durability of the phosphate treatment in real environmental conditions.

REFERENCES

[1] Giorgi, R.; Dei, L.; Baglioni, P. A New Method for Consolidating Wall Paintings Based on Dispersions of Lime in Alcohol, *Stud. Conserv.* **2000**, *45*, 154-161, doi:10.1179/sic.2000.45.3.154

[2] Rodriguez-Navarro, C; Ruiz-Agudo, E. Nanolimes: from synthesis to application. *Pure Appl. Chem.* **2018**, *90*, 523–550, doi: 10.1515/pac-2017-0506

[3] Chelazzi, D.; Poggi, P.; Jaidar, Y.; Toccafondi, N.; Giorgi, R.; Baglioni, P. Hydroxide nanoparticles for cultural heritage: Consolidation and protection of wall paintings and carbonate materials *J. Colloid Interface Sci.* **2013**, *392*, 42–49, doi:10.1016/j.jcis.2012.09.069

[4] Borsoi, G.; Lubelli, B.; van Hees, R.; Veiga, R.; Silva, A.S. Understanding the transport of nanolime consolidants within Maastricht limestone. *J. Cult. Herit.* **2016**, *18*, 242-249, doi:10.1016/j.culher.2015.07.014

[5] Borsoi, G.; Lubelli, B.; van Hees, R.; Veiga, R.; Santos Silva, A.; Colla, L.; Fedele, L.; Tomasin, P. Effect of solvent on nanolime transport within limestone: How to improve in-depth deposition. *Colloid Surface A.* **2016**, *497*, 171–181. doi:10.1016/j.colsurfa.2016.03.007

[6] Otero, J.; Starinieri, V.; Charola, A.E.; Taglieri, G. Influence of different types of solvent on the effectiveness of nanolime treatments on highly porous mortar substrates, *Constr. Build. Mater.* **2020**, *230*, 117112, doi:10.1016/j.conbuildmat.2019.117112

[7] Daniele, V.; Taglieri, G. Nanolime suspensions applied on natural lithotypes: The influence of concentration and residual water content on carbonatation process and on treatment effectiveness. *J. Cult. Herit.* **2010**, *11*, 102-106, doi:10.1016/j.culher.2009.04.001

[8] Rodriguez-Navarro, C.; Vettori, I.; Ruiz-Agudo, E. Kinetics and mechanism of calcium hydroxide conversion into calcium alkoxides: implications in heritage conservation using nanolimes. *Langmuir.* **2016**, *32*, 5183−5194, doi:10.1021/acs.langmuir.6b01065

[9] Licchelli, M.; Malagodi, M.; Weththimuni, M.; Zanchi, C. Nanoparticles for conservation of bio-calcarenite stone, *Appl. Phys. A.* **2014**, *114*, 673-683. doi:10.1007/s00339-013-7973-z

[10] Borsoi, G.; Lubelli, B.; van Hees, R.; Veiga, R.; Silva, A.S. Evaluation of the effectiveness and compatibility of nanolime consolidants with improved properties. *Construct. Building Mater.* **2017**, *142*, 385-394, doi:10.1016/j.conbuildmat.2017.03.097

[11] Ruffolo, S.A.; La Russa, M.F.; Ricca, M.; Belfiore, C.M.; Macchia, A.; Comite, V.; Pezzino, A.; Crisci, G.M. New insights on the consolidation of salt weathered limestone: the case study of Modica stone. *Bull. Eng. Geol. Environ.* **2017**, *76*, 11-20, doi:10.1007/s10064-015-0782-1

[12] Pozo-Antonio, J.S.; Otero, J.; Alonso, P.; Mas i Barberà, X. Nanolime- and nanosilica-based consolidants applied on heated granite and limestone: Effectiveness and durability. *Constr. Build. Mater*. **2019**, *201*, 852–870. doi:10.1016/j.conbuildmat.2018.12.213

[13] Natali, I.; Tomasin, P.; Becherini, F.; Bernardi, A.; Ciantelli, C.; Favaro, M.; Favoni, O.; Forrat Pérez, V.J.; Olteanu, I.D.; Romero Sanchez, M.D.; Vivarelli, A.; Bonazza, A. Innovative consolidating products for stone materials: field exposure tests as a valid approach for assessing durability. *Herit. Sci.* **2015**, *3*, 6. doi:10.1186/s40494-015-0036-3

[14] Bonazza, A.; Vidorni, G.; Natali, I.; Ciantelli, C.; Giosuè, C.; Tittarelli, F. Durability assessment to environmental impact of nano-structured consolidants on Carrara marble by field exposure tests. *Sci. Total Environ*. **2017**, *575*, 23-32. doi: 10.1016/j.scitotenv.2016.10.004

[15] Arizzi, A.; Gomez-Villalba, L.S.; Lopez-Arce, P.; Cultrone, G.; Fort, R. Lime mortar consolidation with nanostructured calcium hydroxide dispersions: the efficacy of different consolidating products for heritage conservation. *Eur. J. Miner*. **2015**, *27*, 311-323, doi:10.1127/ejm/2015/0027-2437

[16] Delgado Rodrigues, J.; Ferreira Pinto, A.P.; Nogueira, R.; Gomes, A. Consolidation of lime mortars with ethyl silicate, nanolime and barium hydroxide. Effectiveness assessment with microdrilling data, *J. Cult. Herit*. **2018**, *29*, 43-53, doi:10.1016/j.culher.2017.07.006

[17] Ambrosi, M.; Dei, L.; Giorgi, R.; Neto, C.; Baglioni, P. Colloidal particles of $Ca(OH)_2$: Properties and applications to restoration of frescoes, Langmuir. 2001, 17, 4251-4255, doi:10.1021/la010269b

[18] Salvatore, A.; Vai, S.; Caporali, S.; Caramelli, D.; Lari, M.; Carretti, E. Evaluation of diammonium hydrogen phosphate and $Ca(OH)_2$ nanoparticles for consolidation of ancient bones. *J. Cult. Herit*. **2020**, *41*, 1-12, doi: 10.1016/j.culher.2019.07.022

[19] Ruffolo, S.A.; La Russa, M.F.; Aloise, P.; Belfiore, C.M.; Macchia, A.; Pezzino, A.; Crisci, G.M. Efficacy of nanolime in restoration procedures of salt weathered limestone rock. *Appl. Phys. A*. **2014**, *114*, 753–758, doi:10.1007/s00339-013-7982-y

[20] Maravelaki-Kalaitzaki, P.; Kallithrakas-Kontos, N.; Korakaki, D.; Agioutantis, Z.; Maurigiannakis, S. Evaluation of silicon-based strengthening agents on porous limestones. *Prog. Org. Coat.* **2006**, *57*, 140-148, doi:10.1016/j.porgcoat.2006.08.007

[21] Scherer, G.W.; Wheeler, G.S. Silicate consolidants for stone. *Key Eng. Mater.* **2009**, *391*, 1–25, doi:10.4028/0-87849-365-4.1.

[22] Zornoza-Indart, A.; Lopez-Arce, P. Silica nanoparticles (SiO_2): Influence of relative humidity in stone consolidation. *J. Cult. Herit.* **2016**, *18*, 258-270, doi:10.1016/j.culher.2015.06.002

[23] Maravelaki-Kalaitzaki, P.; Kallithrakas-Kontos, N.; Agioutantis, Z.; Maurigiannakis, S.; Korakaki, D. A comparative study of porous limestones treated with silicon-based strengthening agents. *Prog. Org. Coat.* **2008**, *62*, 49–60, doi:10.1016/j.porgcoat.2007.09.020

[24] Vasanelli, E.; Calia, A.; Masieri, M.; Baldi, G. Stone consolidation with SiO_2 nanoparticles: Effects on a high porosity limestone. *Constr. Build. Mater*. **2019**, *219*, 154-163. doi:10.1016/j.conbuildmat.2019.05.169

[25] La Russa, M.F.; Ruffolo, S.A.; Ivarez de Buergo, M.A.; Ricca, M.; Belfiore, C.; Pezzino, A.; Crisci, G.M. The behaviour of consolidated Neapolitan yellow Tuff against salt weathering. *Bull. Eng. Geol. Environ.* **2017**, *76*, 115-124, doi: 10.1007/s10064-016-0874-6

[26] Siegesmund, S.; Ullemeyer, K.; Weiss, T.; Tschegg, E.K. Physical weathering of marbles caused by anisotropic thermal expansion. *Int. J. Earth Sci.* **2000**, *89*, 170–182, doi:10.1007/s005310050324

[27] Sassoni, E.; Franzoni, E. Influence of porosity on artificial deterioration of marble and limestone by heating. *Appl. Phys. A*. **2014**, *115*, 809–816, doi:10.1007/s00339-013-7863-4

[28] Sassoni, E.; Franzoni, E. Sugaring marble in the Monumental Cemetery in Bologna (Italy): Characterization of naturally and artificially weathered samples and first results of consolidation by hydroxyapatite. *Appl. Phys. A*. **2014**, *117*, 1893-1906, doi:10.1007/s00339-014-8629-3.

[29] Sassoni, E.; Graziani, G.; Franzoni, E. Repair of sugaring marble by ammonium phosphate: Comparison with ethyl silicate and ammonium oxalate and pilot application to historic artifact. *Mater. Des.* **2015**, *88*, 1145-1157, doi:10.1016/j.matdes.2015.09.101

[30] Sassoni, E.; Andreotti, S.; Scherer, G.W.; Franzoni, E.; Siegesmund, S. Bowing of marble slabs: Can the phenomenon be arrested and prevented by inorganic treatments? *Environ. Earth Sci.* **2018**, *77*, 387, doi:10.1007/s12665-018-7547-7

[31] Skoulikidis, T.; Vassiliou, P.; Tsakona, K. Surface consolidation of Pentelic marble - Criteria for the selection of methods and materials - The Acropolis case, *Environ. Sci. & Pollut. Res.* **2005**, *12*, 28-33, doi:10.1065/espr2004.11.230

[32] Hansen, E.; Dohene, E.; Fidler, J.; Larson, J.; Martin, B.; Matteini, M.; Rodrìguez-Navarro, C.; Pardo, E.S.; Price, C.; de Tagle, A.; Teutonico, J.M.; Weiss, N. A review of selected inorganic consolidants and protective treatments for porous calcareous materials, Reviews in conservation. **2003**, *4*, 13-25

[33] Wheeler, G.S. Alkoxysilanes and the Consolidation of Stone (Research in conservation), The Getty Conservation Institute, Los Angeles, 2005

[34] Verges-Belmin, V.; Orial, G.; Garnier, D.; Bouineau, A.; Coignard, R. Impregnation of badly decayed Carrara marble by consolidating agents: Comparison of seven treatments, In: La conservation des monuments dans le bassin metiterraneen: Actes du 2° symposium international, Geneve, 19-21/11/1991, 1992, 421-437

[35] Sassoni, E.; Naidu, S.; Scherer, G.W. The use of hydroxyapatite as a new inorganic consolidant for damaged carbonate stones. *J. Cult. Herit.* **2011**, *12*, 346-355, doi:10.1016/j.culher.2011.02.005.

[36] Matteini, M.; Rescic, S.; Fratini, F.; Botticelli, G. Ammonium phosphates as consolidating agents for carbonatic stone materials used in architecture and cultural heritage: Preliminary research. *Int. J. Archit. Herit.* **2011**, *5*, 717-736, doi:10.1080/15583058.2010.495445.

[37] Naidu, S.; Scherer, G.W. Nucleation, growth and evolution of calcium phosphate films on calcite. *J. Colloid Interface Sci.* **2014**, *435*, 128–137, doi:10.1016/j.jcis.2014.08.018.

[38] Kamiya, M.; Hatta, J.; Shimada, E.; Ikuma, Y.; Yoshimura, M.; Monma, H. AFM analysis of initial stage of reaction between calcite and phosphate. *Mater. Sci. Eng. B Solid-State Mater. Adv. Technol.* **2004**, *111*, 226–231, doi:10.1016/j.mseb.2004.05.007.

[39] Dorozhkin, S.V. Calcium orthophosphates: Occurrence, properties, biomineralization, pathological calcification and biomimetic applications. *Biomatter.* **2011**, *1*, 121–164, doi:10.4161/biom.18790.

[40] Balonis, M.; Ma, M.; Kakoulli, I. Phase relations in the calcium carbonate/ammonium phosphate system under aqueous conditions and 25°C. *J. Am. Ceram. Soc.* **2020**, *00*, 1-14. doi:10.1111/jace.17047

[41] Possenti, E.; Colombo, C.; Bersani, D.; Bertasa, M.; Botteon, A.; Conti, C.; Lottici, P.P.; Realini, M. New insight on the interaction of diammonium hydrogen phosphate conservation treatment with carbonatic substrates: A multi-analytical approach. *Microchem. J.* **2016**, *127*, 79–86, doi:10.1016/j.microc.2016.02.008.

[42] Possenti, E.; Colombo, C.; Conti, C.; Gigli, L.; Merlini, M.; Rikkert Plaisier, J.; Realini, M.; Sali, D.; Gatta, G.D. Diammonium hydrogenphosphate for the consolidation of building materials. Investigation of newly-formed calcium phosphates. *Constr Build Mater.* **2019**, *195*, 557–563, doi:10.1016/j.conbuildmat.2018.11.077

[43] Franzoni, E.; Sassoni, E.; Graziani, G. Brushing, poultice or immersion? The role of the application technique on the performance of a novel hydroxyapatite-based consolidating treatment for limestone. *J. Cult. Herit.* **2015**, *16*, 173–184, doi:10.1016/j.culher.2014.05.009.

[44] Graziani, G.; Sassoni, E.; Franzoni, E.; Scherer, G.W. Hydroxyapatite coatings for marble protection: Optimization of calcite covering and acid resistance. *Appl. Surf. Sci.* **2016**, *368*, 241–257, doi:10.1016/j.apsusc.2016.01.202.

[45] Sassoni, E.; Graziani, G.; Franzoni, E.; Scherer, G.W. Calcium phosphate coatings for marble conservation: Influence of ethanol and isopropanol addition to the precipitation

medium on the coating microstructure and performance. *Corros. Sci.* **2018**, *136*, 255–267, doi:10.1016/j.corsci.2018.03.019.

[46] Naidu, S.; Sassoni, E.; Scherer, G.W. New treatment for corrosion-resistant coatings for marble and consolidation of limestone. In *Jardins de Pierres—Conservation of Stone in Parks, Gardens and Cemeteries*; Stefanaggi, M., Vergès-Belmin, V., Eds.; XL Print, Paris, France, 2011; pp. 289–294

[47] Naidu, S.; Liu, C.; Scherer, G.W. Hydroxyapatite-based consolidant and the acceleration of hydrolysis of silicate-based consolidants. *J. Cult. Herit.* **2015**, *16*, 94-101, doi:10.1016/j.culher.2014.01.001

[48] Graziani, G.; Sassoni, E.; Franzoni, E.; Consolidation of porous carbonate stones by an innovative phosphate treatment: mechanical strengthening and physical-microstructural compatibility in comparison with TEOS-based treatments. *Heritage Science.* **2015**, *3*, 1-6, doi: 10.1186/s40494-014-0031-0

[49] Sassoni, E.; Graziani, G.; Franzoni, E. An innovative phosphate-based consolidant for limestone. Part 1: Effectiveness and compatibility in comparison with ethyl silicate. *Construct. Build. Mater.* **2016**, *102*, 918–930, doi:10.1016/j.conbuildmat.2015.04.026.

[50] Sassoni, E.; Graziani, G.; Franzoni, E. An innovative phosphate-based consolidant for limestone. Part 2: Durability in comparison with ethyl silicate. *Construct. Build. Mater.* **2016**, *102*, 931–942, doi:10.1016/j.conbuildmat.2015.10.202.

[51] Molina, E.; Rueda-Quero, L.; Benavente, D.; Burgos-Cara, A.; Ruiz-Agudo, E.; Cultrone, G. Gypsum crust as a source of calcium for the consolidation of carbonate stones using a calcium phosphate-based consolidant. *Constr. Build. Mater*. **2017**, *143*, 298–311, doi:10.1016/j.conbuildmat.2017.03.155.

[52] Sassoni, E.; Franzoni, E.; Pigino, B.; Scherer, G.W.; Naidu, S. Consolidation of calcareous and siliceous sandstones by hydroxyapatite: Comparison with a TEOS-based consolidant. *J. Cult. Herit.* **2013**, *14*, e103–e108, doi:10.1016/j.culher.2012.11.029.

[53] Molina, E.; Fiol, C.; Cultrone, G. Assessment of the efficacy of ethyl silicate and dibasic ammonium phosphate consolidants in improving the durability of two building sandstones from Andalusia (Spain), *Environ. Earth Sci.* **2018**, *77*, 302, doi:10.1007/s12665-018-7491-6

[54] Balonis-Sant, M.; Ma, X.; Kakoulli, I. Preliminary results on biomimetic methods based on soluble ammonium phosphate precursors for the consolidation of archaeological wall paintings. In *Archaeological Chemistry VIII*, ACS Symposium Series; American Chemical Society: Washington, DC, USA, 2013; Volume 1147, pp. 419–447, doi:10.1021/bk-2013-1147.ch022.

[55] Sassoni, E.; Franzoni, E. Lime and cement mortar consolidation by ammonium phosphate. *Constr. Build. Mater*. **2020**, *245*, 118409, doi:10.1016/j.conbuildmat.2020.118409

[56] Sassoni, E.; Graziani, G.; Franzoni, E.; Scherer, G.W. Conversion of calcium sulfate dihydrate into calcium phosphates as a route for conservation of gypsum stuccoes and sulfated marble. *Construct. Build. Mater.* **2018**, *170*, 290–301, doi:10.1016/j.conbuildmat.2018.03.075.

[57] Wang, L.; Wang, J.; Xu, Y.; Chen, P.; Yuan, J.; Qian, X. Novel surface treatment of concrete bricks using acid-resistance mineral precipitation. *Constr. Build. Mater*. **2018**, *162*, 265-271, doi: 10.1016/j.conbuildmat.2017.12.019

[58] North, A.; Balonis, M.; Kakoulli, I. Biomimetic hydroxyapatite as a new consolidating agent for archaeological bone. *Stud. Conserv*. **2016**, *61*, 146-161, doi:10.1179/2047058415Y.0000000020.

[59] Yang, F.; He, D.; Liu, Y.; Li, N.; Wang, Z.; Ma, Q.; Dong, G. Conservation of bone relics using hydroxyapatite as protective material. *Appl. Phys. A* **2016**, *122*, 479, doi:10.1007/s00339-016-0015-x.

[60] Shekofteh, A.; Molina, E.; Rueda-Quero, L.; Arizzi, A.; Cultrone, G. The efficiency of nanolime and dibasic ammonium phosphate in the consolidation of beige limestone from the

Pasargadae World Heritage Site. Archaeol Anthrop Sci, **2019**, doi:10.1007/s12520-019-00863-y

[61] Yang, F.W.; Liu, Y.; Zhu, Y.C.; Long, S.J.; Zuo, G.F.; Wang, C.Q.; Guo, F.; Zhang, B.J.; Jiang, S.W. Conservation of weathered historic sandstone with biomimetic apatite. *Chin. Sci. Bull.* **2012**, *57*, 2171–2176, doi:10.1007/s11434-012-5039-9

[62] Weththimuni, M.L.; Licchelli, M.; Malagodi, M.; Rovella, N.; La Russa, M. Consolidation of bio-calcarenite stone by treatment based on diammonium hydrogen phosphate and calcium hydroxide nanoparticles, *Measurement*. **2018**, *127*, 396–405, doi: 10.1016/j.measurement.2018.06.007

[63] Masi, G.; Sassoni, E. Comparison between ammonium phosphate and nanolimes for render consolidation, *IOP Conf. Ser. Mater. Sci. Eng.* (in press)

[64] Sassoni, E.; Hydroxyapatite and Other Calcium Phosphates for the Conservation of Cultural Heritage: A Review. *Materials*. **2018**, *11*, 557, doi:10.3390/ma11040557

[65] Murru, A.; Fort, R. Diammonium hydrogen phosphate (DAP) as a consolidant in carbonate stones: Impact of application methods on effectiveness, *J. Cultur. Herit.* **2019**, doi:10.1016/j.culher.2019.09.003

[66] Naidu, S.; Blair, J.; Scherer, G.W. Acid-resistant coatings on marble. *J. Am. Ceram. Soc.* **2016**, *99*, 3421–3428, doi:10.1111/jace.14355.

[67] Graziani, G.; Sassoni, E.; Scherer, G.W.; Franzoni, E. Resistance to simulated rain of hydroxyapatite- and calcium oxalate-based coatings for protection of marble against corrosion. *Corros. Sci.* **2017**, *127*, 168–174, doi:10.1016/j.corsci.2017.08.020.

[68] Sassoni, E.; Franzoni, E.; Stefanova, M.; Kamenarov, Z.; Scopece, P.; Verga Falzacappa, E. Comparative study between ammonium phosphate and ethyl silicate towards conservation of prehistoric paintings in the Magura cave (Bulgaria). *Coatings*. **2020**, *10*, 250; doi:10.3390/coatings10030250

[69] Matteini, M.; Colombo, C.; Botticelli, G.; Casati, M.; Conti, C.; Negrotti, R.; Possenti, E.; Realini, M. Ammonium phosphates to consolidate carbonatic stone materials: An inorganic-mineral treatment greatly promising. In Built Heritage 2013 Monitoring Conservation Management; Boriani, M., Gabaglio, R., Gulotta, D., Eds.; Politecnico di Milano: Milan, Italy, **2013**; pp. 1278-1286.

[70] Barriuso, B.C.; Botticelli, G.; Cuzman, O.A.; Osticioli, I.; Tiano, P.; Matteini, M. Conservation of calcareous stone monuments: Screening different diammonium phosphate based formulations for countering phototrophic colonization. *J. Cult. Herit*. **2017**, *27*, 97-106, doi: 10.1016/j.culher.2017.03.002

[71] Ma, X.; Balonis, M.; Pasco, H.; Toumazou, M.; Counts, D.; Kakoulli, I. Evaluation of hydroxyapatite effects for the consolidation of a Hellenistic-Roman rock-cut chamber tomb at Athienou-Malloura in Cyprus. *Construct. Build. Mater.* **2017**, *150*, 333–344, doi:10.1016/j.conbuildmat.2017.06.012.

[72] Scherer, G.W.; Franzoni, E.; Sassoni, E.; Graziani, G. Phosphate consolidants for carbonate stones, *APT Bulletin: The Journal of Preservation Technology*. **2018**, *49*, 61-68, https://www.jstor.org/stable/26502504

[73] Moropoulou, A.; Haralampopoulos, G.; Tsiourva, Th.; Auger, F.; Birginie M. Artificial weathering and non-destructive tests for the performance evaluation of consolidation materials applied on porous stones, *Mater. Struct.* **2003**, *36*, 210-217, doi: 10.1007/BF02479613

[74] Pinna, D.; Salvadori, B.; Porcinai, S. Evaluation of the application conditions of artificial protection treatments on salt-laden limestones and marble. *Construct. Build. Mater*. **2011**, *25*, 2723–2732, doi:10.1016/j.conbuildmat.2010.12.023

[75] Doherty, B.; Pamplona, M.; Miliani, C.; Matteini, M.; Sgamellotti, A.; Brunetti, B. Durability of the artificial calcium oxalate protective on two Florentine monuments. *J. Cult. Herit.* **2007**, *8*, 186-192, doi:10.1016/j.culher.2006.12.002

[76] Charola, A.E.; Centeno, S.A.; Normandin, K. The New York Public Library: Protective treatment for sugaring marble, *J. Archit. Conserv.* **2010**, *16*, 29-44, doi: 10.1080/13556207.2010.10785068

[77] Sandrolini, F.; Franzoni, E.; Sassoni, E.; Diotallevi, P.P. The contribution of urban-scale environmental monitoring to materials diagnostics: a study on the Cathedral of Modena (Italy). *J. Cult. Herit.* **2011**, *12*, 441-450, doi:10.1016/j.culher.2011.04.005

[78] Dreyfuss, T. Interactions on site between powdering porous limestone, natural salt mixtures and applied ammonium oxalate. *Herit. Sci.* **2019**, *7*, 5. doi:10.1186/s40494-019-0247-0

[79] Kollwitz, J.; Herdejurgen, H. Die ravennatischen Sarkophage, Die Sarkophage der westlichen Gebiete des Imperium Romanum 8, Gebr. Mann, Berlin, **1979**

[80] Attanasio, D.; Brilli, M.; Bruno, M. The properties and identification of marble from Proconnesos (Marmara Island, Turkey): A new database including isotopic, EPR and petrographic data. *Archaeometry*. **2008**, *50*, 747–774, doi:10.1111/j.1475-4754.2007.00364.x

[81] Moropoulou, A.; Delegou, E.T.; Apostolopoulou, M.; Kolaiti, A.; Papatrechas, C.; Economou, G.; Mavrogonatos, G. The white marbles of the Tomb of Christ in Jerusalem: Characterization and provenance. *Sustainability*. **2019**, *11*, 2495; doi:10.3390/su11092495

[82] Sassoni, E.; Phosphate-based treatments for conservation of stone, *RILEM Technical Letters*. **2017**, *2*, 14-19, doi:10.21809/rilemtechlett.2017.34

[83] Graziani, G.; Colombo, C.; Conti, C.; Possenti, E.; Perelli Cippo, E.; Realini, M.; Sassoni, E. Neutron radiography as a tool for assessing penetration depth and distribution of a phosphate consolidant for limestone, *Constr. Build. Mater.* **2018**, *187*, 238-247, doi:10.1016/j.conbuildmat.2018.07.173

[84] Weiss, T.; Rasolofosaon, P.N.J.; Siegesmund, S. Ultrasonic wave velocities as a diagnostic tool for the quality assessment of marble; in Natural stone, weathering phenomena, conservation strategies and case studies. Geological Society, London, Special Publications, **2002**, *205*, 149-164

[85] Luque, A.; Ruiz-Agudo, E.; Cultrone, G.; Sebastiàn, E.; Siegesmund, S. Direct observation of microcrack development in marble caused by thermal weathering, *Environ. Earth Sci.* **2011**, *62*, 1375-1386, doi:10.1007/s12665-010-0624-1

[86] Ruedrich, J.; Knell, C.; Enseleit, J.; Rieffel, Y.; Siegesmund, S. Stability assessment of marble statuaries of the Schlossbrucke (Berlin, Germany) based on rock strength measurements and ultrasonic wave velocities, *Environ. Earth. Sci.* **2013**, *69*, 1451–1469, doi:10.1007/s12665-013-2246-x

[87] European Standard EN 15801, Conservation of cultural property - Test methods - Determination of water absorption by capillarity, 2010

[88] Tao, J. FTIR and Raman Studies of Structure and Bonding in Mineral and Organic–Mineral Composites, *Methods Enzymol*, **2013**, *532*, 533-56. doi:10.1016/B978-0-12-416617-2.00022-9

[89] Parker, J. E.; Thompson, S. P.; Lennie, A. R.; Potter, J.; Tang, C. C. A study of the aragonite-calcite transformation using Raman spectroscopy, synchrotron powder diffraction and scanning electron microscopy. *CrystEngComm*. **2010**, *12*, 1590–1599, doi:10.1039/b921487a

[90] Rodriguez-Navarro, C.; Elert, K.; Ševčík, R. Amorphous and crystalline calcium carbonate phases during carbonation of nanolimes: implications in heritage conservation, *CrystEngComm*. **2016**, *18*, 6594, doi:10.1039/c6ce01202g

[91] Rubio, F.; Rubio, J.; Oteo, J.L. A FT-IR study of the hydrolysis of Tetraethylorthoselicate (TEOS), *Spectrosc. Lett*. **1998**, *31*, 199-219, doi:10.1080/00387019808006772

[92] Sassoni, E.; Graziani, G.; Ridolfi, G.; Bignozzi, M.C.; Franzoni, E. Thermal behavior of Carrara marble after consolidation by ammonium phosphate, ammonium oxalate and ethyl silicate. *Mater. Des*. **2017**, *120*, 345–353, doi:10.1016/j.matdes.2017.02.040.

[93] Karampas, I.A.; Kontoyannis, C.G. Characterization of calcium phosphates mixtures. *Vib Spectrosc*. **2013**, *64*,126– 133, doi:10.1016/j.vibspec.2012.11.003

[94] Evans, A.G.; Drory, M.D.; Hu, M.S. The cracking and decohesion of thin films, *J. Mater. Res.* **1988**, *3*, 1043-1049. doi:10.1557/JMR.1988.1043

[95] Graziani, G.; Sassoni, E.; Scherer, G.W.; Franzoni, E. Penetration depth and redistribution of an aqueous ammonium phosphate solution used for porous limestone consolidation by brushing and immersion. *Construct. Build. Mater*. **2017**, *148*, 571–578, doi:10.1016/j.conbuildmat.2017.05.097.

[96] Köhler, W. Preservation problems of Carrara marble sculptures: Potsdam-Sanssouci ("radical structural destruction" of Carrara marble). **1988**. VI International Congress on Deterioration and Conservation of Stone, Proc Actes, 653-662

[97] Sharma, G. Color fundamentals for digital imaging. In *Digital Color Imagining Handbook*; CRC Press: Boca Raton, FL, USA, 2003

[98] Delgado Rodrigues, J.; Grossi, A. Indicators and ratings for the compatibility assessment of conservation actions. *J. Cult. Herit.* **2007**, *8*, 32–43, doi:10.1016/j.culher.2006.04.007
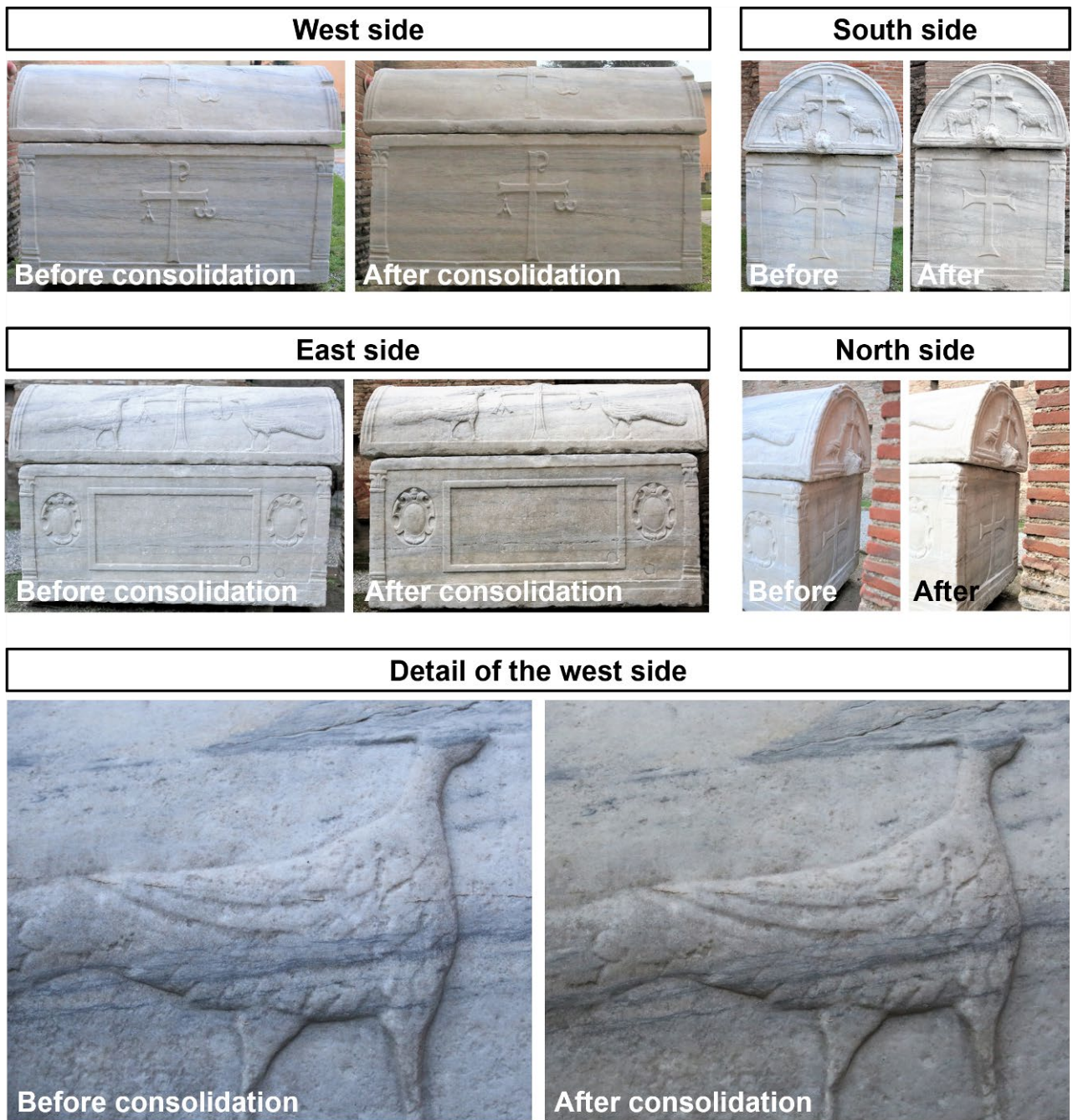
Figure S1. Consolidation of the sarcophagus by ammonium phosphate: (1) application of Japanese paper onto the marble surface by wetting with the DAP solution; (2) application of the poultice imbibed with the DAP solution; (3) wrapping with a polyethylene film to prevent evaporation; (4) removal of the poultice after 24 hours; (5) view of the cover after application of the poultice; (6) view of the cover after wrapping with the polyethylene film; (7) application of the poultice onto the lower part of the sarcophagus.
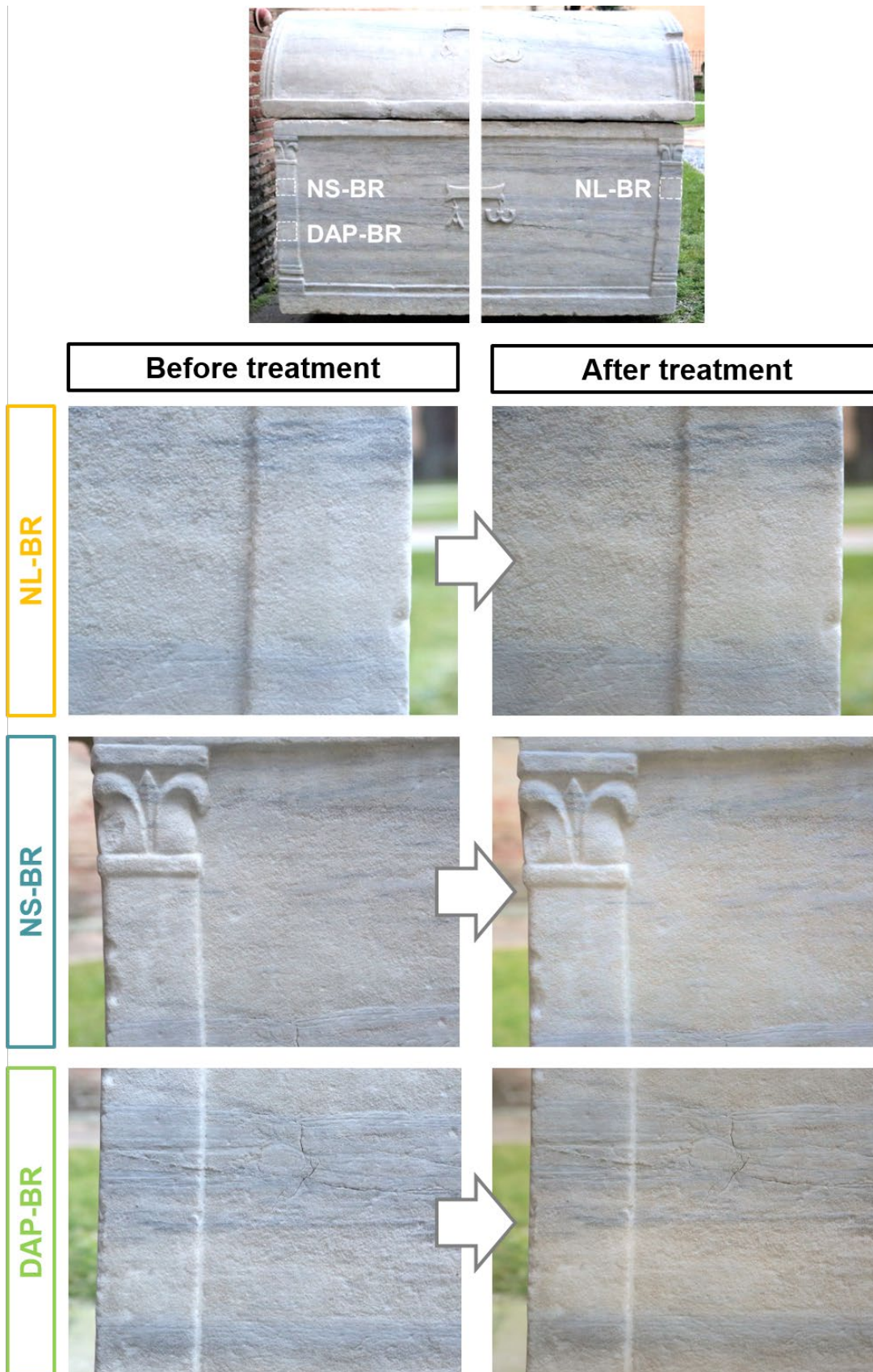
Figure S2. Aesthetic appearance of the test areas before and after consolidation with "NL-BR", "NS-BR" and "DAP-BR". The difference in lighting owing to the different time and period of the year when the photos were taken, before and after consolidation, makes it difficult to evaluate the overall chromatic alteration, but it is possible to notice the absence of any white hazes or surface staining.

Figure S3. Aesthetic appearance of the four sides of the sarcophagus before and after consolidation with "DAP-POUL". The difference in lighting owing to the different time and period of the year when the photos were taken, before and after consolidation, makes it difficult to evaluate the overall chromatic alteration, but it is possible to notice the absence of any white hazes or surface staining.